ISSN: 1863-5598

ZKZ 64717
01-12

Bodo´s Power Systems®

Electronics in Motion and Conversion

January 2012

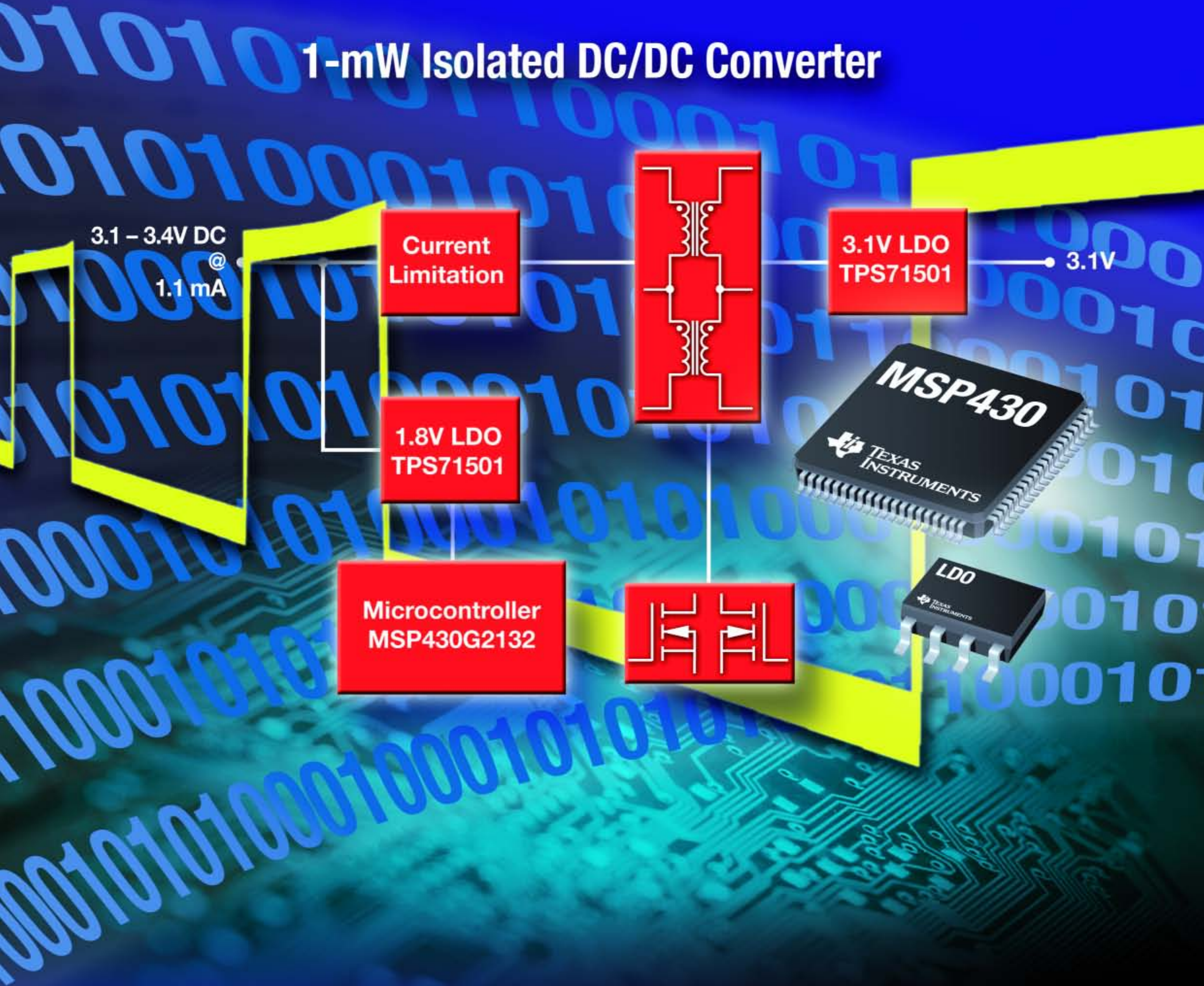

Bodo´s Power Systems®

Bodo´s Power Systems®

The Gallery

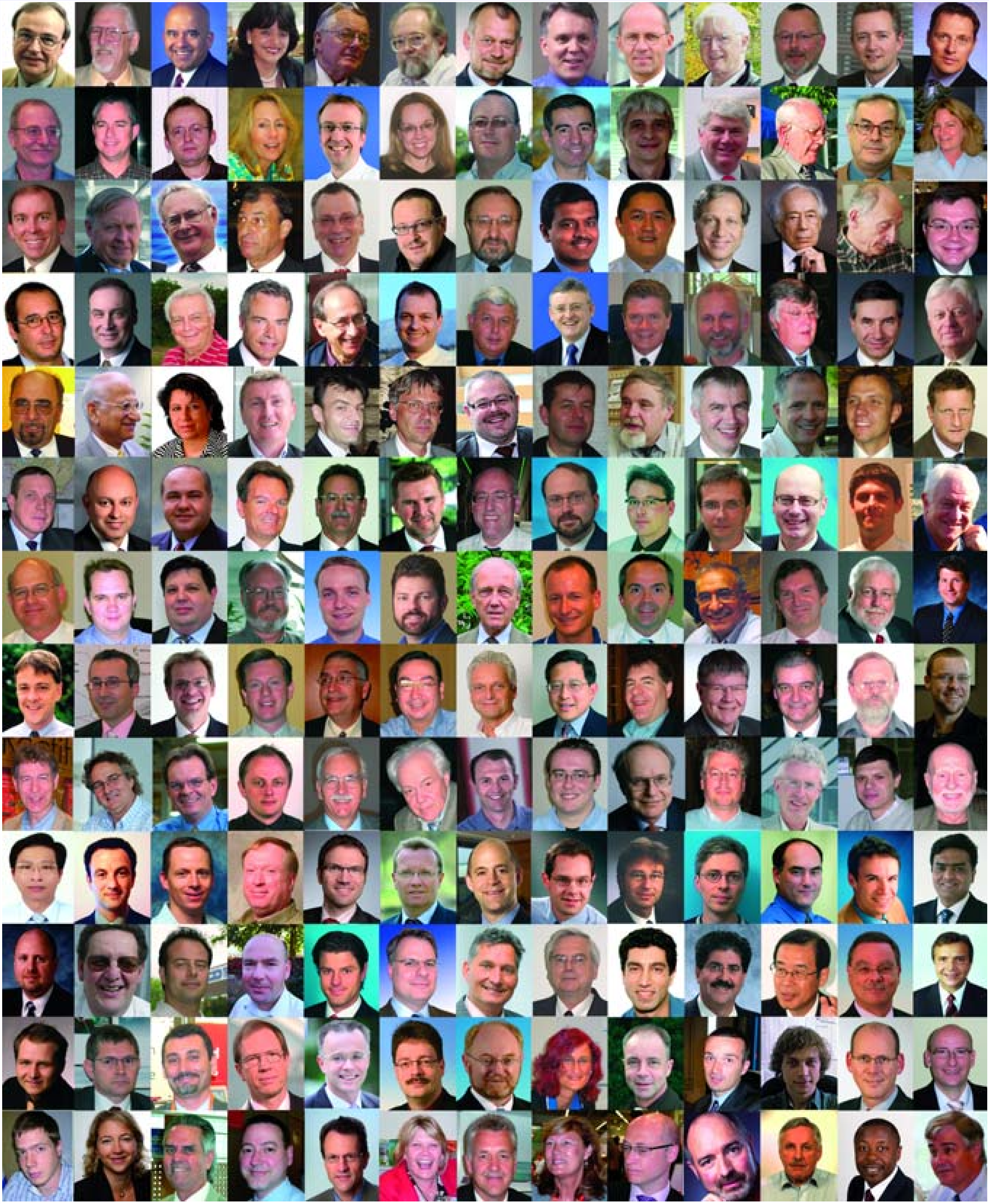

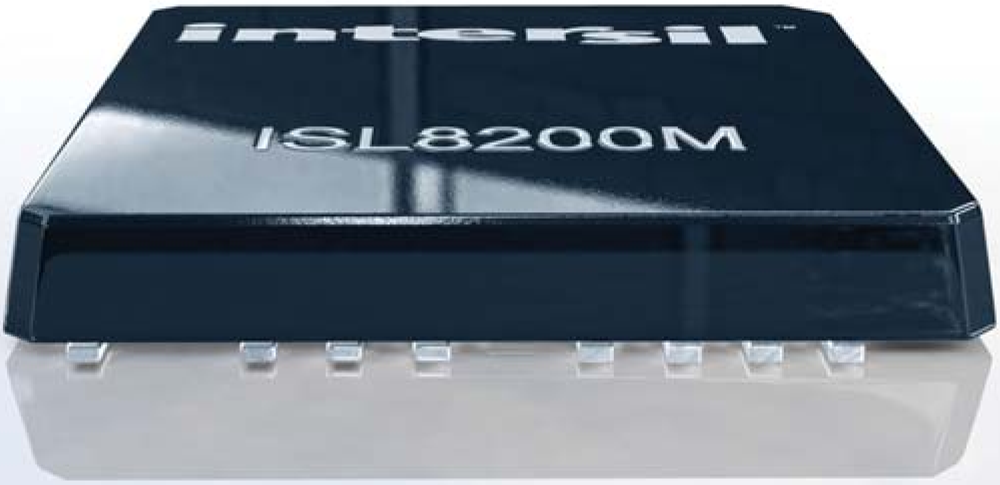
intersil
ISL8200M

Bodo´s Power Systems®

A Media
Katzbek 17a
D-24235 Laboe, Germany
Phone: +49 4343 42 17 90
Fax: +49 4343 42 17 89
editor@bodospower.com
www.bodospower.com

Publishing Editor
Bodo Arlt, *Dipl.-Ing.*
editor@bodospower.com

Creative Direction & Production
Repro Studio Peschke
Repro.Peschke@t-online.de

Free Subscription to qualified readers

Bodo´s Power Systems
is available for the following
subscription charges:
Annual charge (12 issues) is 150 €
world wide
Single issue is 18 €
subscription@bodospower.com

circulation ASC audit since 09/2006 print run 20 000

Printing by:
Central-Druck Trost GmbH & Co
Heusenstamm, Germany

Events

Green Building,
San Jose CA,
Jan. 23rd-25th
http://greenbuildingpower.darnell.com

Smart Grids Summit
Stockholm,
Jan. 24th -25th
www.thesmartgridsummit.com

APEC,
Orlando, Florida,
Feb. 5th -9th
http://apec-conf.org

EMC,
Düsseldorf, Germany,
Feb. 7th -9th
www.mesago.de/en/EMV/main.htm

Embedded world,
Nuremberg, Germany,
Feb 28th- March 1st
www.embedded-world.de

Motivation and Inspiration

Visiting California in December and seeing the Disney Museum gave me impressions of a man that changed a lot in the world. Walt Disney grew up in an environment that supported him and guided his cartoon painting. An Aunt provided paper and pencils and the motivation to try. What resulted is recognized all over the world. That is what we can all deliver to children – encouraging them in creative activities, guiding their development to choose a profession that will capture their excitement and, at the same time, provide for their needs. Too many people work just for the money but being happy in your work provides much more than money. It is only one life for each of us and we should do it right and help our children with theirs. If we get them motivated to become an engineer, we have achieved a great task.

Walt Disney also had a steam train going around his house. It is on display in San Francisco in the museum. Trains have been a magic potion in the lives of many successful men. In talking to a number of leaders in industry, they make no secret of their fascination for model trains. The magic is still alive.

Technology has moved on from Disney’s days and seeing the tall, mechanically operated, trick film movie camera was very impressive. This was the production center for all the magic films we saw a children. These days, computers do the animation and stand-along film is nearly obsolete having been replaced by digital cameras in all kind of applications.

Walt Disney also provided the vision for Disney World in Orlando, Florida. APEC, the most visionary power conference and show in North America, will take place at Disney World in early February. It is practically a must-see to gauge progress in Power Electronic Technology – a place where experts from science and industry come together and join in conversation in the inspiring atmosphere of a man with great ideas and the faith to see them through to completion.

Communication is the only way to progress. We delivered twelve issues last year and this year we will continue on time, every time. As a media partner, Bodo’s Power Systems is internationally positioned.

My Green Power Tip for January:
Santa may have brought you a nice new coat. Give your old warm coats to people that might need them for the winter. That is much better than throwing them away. The Salvation Army will take them for distribution to where your gift will be appreciated.

See you at APEC

Best regards


Future precision.
Future performance.
Now available.
LEM
CAS 6-NP

Power Semiconductor Application Manual

Semikron presents the English version of its Application Manual. The German version is already available. The 464-page-long manual provides electronics experts with detailed information on the selection and use of IGBT, MOSFET, diode and thyristor components.

The Application Manual contains detailed application-related information such as electrical configuration for key operating conditions, driver and protection elements for semiconductors, thermal dimensioning and cooling, tips on parallel and series connection, assembly tips for optimised power layouts with regard to parasitic elements, as well as notes to help users better understand datasheets and the requirements that arise from specific ambient conditions. Assembly and connection technologies which have a major impact on the properties of semiconductor modules and the limits in field applications are also described, as are reliability data, life cycle analyses and key test processes.

The German and English Application Manual is available for €9.90 under the ISBN No. 978-3-938843-56-7 (German) and under ISBN-Nr. 978-3-938843-66-6 (English) and via the Sindopower power electronics eCommerce portal at www.sindopower.com. Based on the Power Electronics Application Manual, excerpts are published on the knowledge platform www.powerelectronics-base.com and www.leistungselektronik-wissen.de, in both German and English. 20 articles are already available and a valuable power electronics reference for amateurs and professionals alike.

“The affordable price makes this work accessible to a multitude of users”, comments Dr. Arendt Wintrich, one of the four authors of the manual and specialist for applications and simulations at Semikron. The three co-authors are Dr.-Ing. Ulrich Nicolai, Dr. techn. Werner Tursky from Semikron, and University Professor Dr.-Ing. Tobias Reimann, head of Industrial Electronics at the Technical University of Ilmenau.

www.semikron.com

Push into Energy harvesting Market

PulseSwitch Systems, LC, which announced that it will begin a strong push into the self-powered switch control and sensor market in 2012, has expanded its Board in preparation for that undertaking. PulseSwitch sells self-powered wireless devices and controls a portfolio of intellectual property relating to self-powered switches, controls, sensors and systems that includes issued patents in more than 25 countries, and pending patent applications in the United States, Canada, Europe, India and China.

Joining PulseSwitch as a consultant and a Board Member will be Donald R. Schroeder, recently retired Executive Vice President of CTS Corporation. During his almost 40 years with CTS, Mr. Schroeder served as Vice President of Sales and Marketing, producing $500M+ in annual sales during his tenure. He was also the President & General Manager of CTS' Electronics Manufacturing Services business and its Electronic Components business with operations in North America, Asia and Europe.

When he was Chief Technology Officer of CTS, Mr. Schroeder negotiated numerous patent licenses with large international corporations. Mr. Schroeder is a Director of IPC, which he also serves as Secretary/Treasurer and the chair of the Marketing and Technology committee.

www.LightningSwitch.com

Texas Instruments Reigns Supreme in Industrial Electronics

Texas Instruments in 2010 was the undisputed champion of a critical electronics market that generates copious growth—but garners little attention: the industrial electronics semiconductor space, according to a new IHS iSuppli Industrial Electronics Market Tracker report from information and analysis provider IHS (NYSE: IHS).

Rank	Company	Revenue in US Dollars	Market Share (%)
1	Texas Instruments	$1.788	6,5%
2	STMicroelectronics	$1.592	5,8%
3	Infineon Technologies	$1.418	5,2%
4	Intel	$1.205	4,4%
5	Analog Devices	$1.188	4,3%
6	Renesas	$952	3,5%
7	Toshiba	$948	3,5%
8	NXP Semiconductors	$845	3,1%
9	Maxim Integrated Products	$779	2,8%
10	Mitsubishi	$753	2,7%

Leveraging its broad participation in a variety of market segments, TI in 2010 earned $1.79 billion in industrial electronics semiconductor revenue, giving it a 6.5 percent market share as presented in the figure below.

“While much attention is heaped on sexier semiconductor markets such as a wireless, computers and consumer electronics, the industrial segment actually outgrew all these areas in 2010,” noted Jacobo Carrasco Heres, industrial electronics analyst at IHS. “In fact, industrial electronics in 2010 was the second-fastest growing semiconductor market after automotive. Dallas-based TI managed to lead in this area last year partly because of its robust footprint worldwide and its broad participation in virtually every industrial electronics market segment—from automation to medical, to energy and military. The company also benefitted from its strong product offerings in analog, microcontrollers and digital signal processing.”

The completion of the acquisition of National Semiconductor in the third quarter this year is expected to further reinforce TI’s hold on the pinnacle when rankings are reassessed at the end of 2011.

www.ihs.com

High efficiency by 3-Level Topology

650V 3-Level-IGBT-Modules with PressFIT-Technology

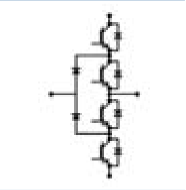

Infineon‘s new family of 3-Level Inverter modules offers significant advantages for designing highly efficient UPS and solar inverters.

the three level inverter proves to be an attractive candidate for low and medium power low voltage applications which require high switching frequencies, complex filtering and high efficiency like double conversion UPS and solar inverters. Integrating all elements of

a phase leg into one module optimizes stray inductance and handling efforts.

- 30A - 400A/650V modules
- Low inductive design
- High reliability due to PressFIT
- Optimized thermal performance
- RoHS compliant

Infineon Technologies Industrial Power, 1050 Route 22, Lebanon, NJ 08833
Phone: 908-236-5600, info.usa@infineon.com

[www.infineon.com/highpower]

Technology Expert to Host Webinar on Head-in-Pillow Elimination

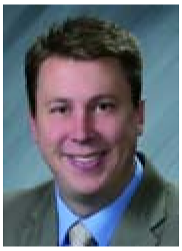

Indium Corporation Product Manager of PCB Assembly Materials Tim Jensen will present Material and Process Optimization for Head-in-Pillow Elimination as part of SMTA's webinar series January 12, 2012, from 11 a.m. to 12:30 p.m.

Tim's presentation will include an overview on Head-in-Pillow (HIP) defects and how process and material selection can have a significant impact on the potential for HIP defects. Tim will also analyze the printing and reflow processes for ways that optimization can help to significantly reduce the potential for HIP, including the critical solder paste attributes that can help minimize HIP.

As a product manager, Tim works with customers to troubleshoot and optimize SMT process lines. He specializes in Sn/Pb and Pb-free solder paste, halogen-free soldering materials, wave solder fluxes, bar solder, rework fluxes, and flux-cored wire.

Tim is an SMTA-certified process engineer and has earned his bachelor's degree in Chemical Engineering from Clarkson University. He readily shares his expertise by authoring technical papers, writing for technical publications, and participates actively in several IPC standards development committees. Tim also authors a blog, which can be found at blogs.indium.com/blog/tim-jensen.

For more information or to register, visit www.smta.org.

Indium Corporation is a premier materials supplier to the global electronics, semiconductor, solar, thin-film and thermal management markets. Products include solders, preforms, and fluxes; brazes; sputter targets; indium, gallium, and germanium chemicals and sourcing; and Reactive NanoFoil®. Founded in 1934, Indium has global technical support and factories located in China, Singapore, South Korea, the United Kingdom, and the USA.

www.indium.com

Employees Perform the Biggest Reforestation in the History of Spain

By planting 7,500 trees of a species threatened with extinction in the Punto Umbria region in Spain, around 1,000 employees of EBV Elektronik, an Avnet company and the leading specialist in Europe, Middle East and Africa semiconductor distribution, left a green mark on Andalusia and showed just how seriously it takes its corporate environmental program ECOmise it™.

With EBV's complete workforce from EMEA coming together in Huelva for a sales conference and team-building event, management realised right from the start how important it was to organize this meeting in a climate-friendly manner. Bernd Schlemmer, director communications of EBV Elektronik, explains the background: "Since we flew all our 1,000 employees to Spain, the terms of our ECOmise it program mean that we felt obliged to compensate not only for our CO^2 consumption through travel, but also to create something sustainable which helps reduce the area's carbon footprint on a long term basis. With this in mind, all employees present participated in this huge project, in which we reforested an area of more than 500.000 m^2 - an area roughly equivalent to 70 football pitches."

Reforestation took place in an area known as 'Los Enebrales', which was declared a natural park in 1989 and is the second biggest nature reserve in the province of Huelva. Los Enebrales' 162 hectares of dunes along the beaches between Punta Umbría and El Portil are covered with pine, bushes and rockroses, as well as seaside junipers, which – despite being the most significant tree in this region – are considered endangered in Andalusia and included on the national Spanish catalogue of species in danger of extinction.

Over a nominal timeframe of 20 years, up to 1,390 tons of CO2 will be absorbed annually through EBV's environmentally- friendly activities; this makes the reforestation program a milestone for corporate social responsibility initiatives in Spain, where a project of this nature has never been carried out on such a large scale before. Meanwhile this reforestation initiative gave the EBV employees involved the opportunity to acquire a profound knowledge of the local flora, heightening their environmental awareness and making for an unforgettable experience. Most importantly, EBV staff left Andalusia greener than they found it.

www.ebv.com

Worldwide Distributor Agreement to Expand Support for RF Systems Designers

Analog Devices announced that it has entered into a worldwide sales distribution agreement with Richardson RFPD, Inc. As one of the leading distributors of RF and microwave components, Richardson RFPD will support the design-in of ADI's high-performance RF ICs (integrated circuits) along with the company's full range of analog, mixed-signal and digital signal-processing products. ADI's RF ICs and signal-processing technology are available now through Richardson RFPD's North and South America offices and are expected to be available through Richardson RFPD's offices in Europe, Middle East, Greater China, Asia Pacific and Japan in the first half of 2012.

ADI delivers world-leading data converters, amplifiers, MEMs, DSPs (digital signal processors) and power management ICs and a portfolio of high-performance RF ICs covering the entire RF signal chain from leading function blocks such as PLLs, mixers and power detectors, to highly integrated short-range single-chip transceiver solutions. Together, these technologies form a complete design and play a fundamental role in converting, conditioning, and processing real-world phenomena in a wide array of applications.

"Our customers are integrating wired and wireless connectivity into an ever-widening range of applications, and ADI's high-performance RF and signal-processing portfolio is at the core of these systems," said Peter Real, ADI vice president for Linear and RF. "With our portfolio and Richardson RFPD's technical team, customers can expect to accomplish great things."

Alex Glass, ADI vice president, worldwide channel sales, said, "We are pleased to enter into this agreement with Richardson RFPD whose highly skilled RF and microwave sales and technical support teams will be accessible to customers through a global network of 47 offices and seven stocking locations."

"We are excited to partner with ADI, and this distributor agreement further elevates Richardson RFPD's ability to support all aspects of our customers' needs for design, logistics, and new product updates," said Greg Peloquin, president of Richardson RFPD. "Combining ADI's leadership position in ADC and DAC technology, and their investment in developing innovative RF products with our global reach into the RF & Wireless market, make it possible for RF engineers to now procure almost every part they need from one qualified source."

www.richardsonrfpd.com

Econo-IGBTs

The 6-PACKs

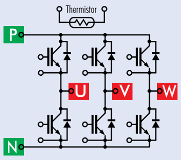

With soldering pins

	I_C	600V	1200V	1700V
45x107,5mm	50A		●	
	75A	●	●	
	100A	●	●	
62 x 122 mm	75A		●	
	100A		●	●
	150A	●	●	●
	180A		●	
	200A		●	

With PressFit contacts

	I_C	600V	1200V
45x107,5mm	50A		●
	75A	●	●
	100A	●	●
62 x 122 mm	100A		●
	150A	●	●
	180A		●
	200A		●

The PIMs

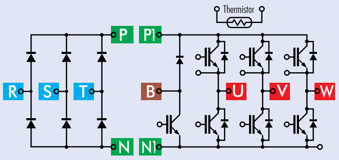

With soldering pins

	I_C	600V	1200V
45x107,5mm	25A		●
	35A		●
	50A	●	●
62 x 122 mm	75A	●	●
	100A	●	●
	150A	●	●

With PressFit contacts

	I_C	600V	1200V
45x107,5mm	25A		●
	35A		●
	50A	●	●
62 x 122 mm	75A	●	●
	100A	●	●
	150A	●	●

The High Power 6-PACKs

	I_C	1200V	1700V
150 x 162 mm	225A	●	●
	300A	●	●
	450A	●	●
	550A	●	

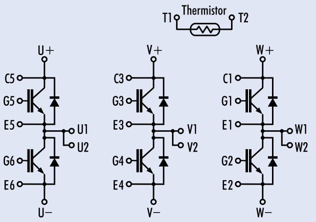

FUJI ELECTRIC EUROPE
e-Front runners

Fuji Electric Europe GmbH
Goethering 58 · 63067 Offenbach am Main · Germany
Fon +49 (069) - 66 90 29 0 · Fax +49(0)69 - 66 90 29 56
semi-info@fujielectric.de . **www.fujielectric.de**
Products Overview ▸ **www.fujielectric-europe.de/info/overview.pdf**

2012 Global Energy Prize Now Accepting Nominations

The Global Energy Prize, one of the world's most respected awards in energy science, is now accepting nominations for its over $1 million 2012 award. The Prize will be given to the winner by the President of Russia in an official ceremony which will take place as part of the St Petersburg International Economic Forum, in June 2012.

The Global Energy Prize annually rewards innovation and solutions in global energy research and its concurrent environmental challenges. The degree to which a development contributes to the benefit of humanity is a key driver in deciding the recipient of the prize. The Prize has become increasingly important as governments, energy companies and consumers all seek to address existing and projected energy shortfalls.

Dr. Arthur Rosenfeld (USA), Laureate of the Global Energy Prize 2011, comments:

"My reaction to the news that I had received the Global Energy Prize was a mixture of delight and complete surprise. My reputation among Americans and other Westerners is fairly well established, but I am almost unknown among Russians who have, until President Medvedev, not paid much attention to my chosen field of efficient use of energy. Thus my selection suggests to me a very flexible process in which Russians are putting a new emphasis on modern energy and environmental policies."

Applications open in November 2011 and will be accepted through February 29th, 2011. Candidates can be nominated only by the highest-rated scientists, such as Nobel Prize Laureates for physics or chemistry, past Laureates of the Global Energy Prize, and Laureates of the Kyoto, Max Planck, Wolf and Balzan prizes.

The winner of the 2012 Prize will be selected by an International Prize Award Committee, which includes 37 internationally-based scientists and specialists, as well as representatives of international research organisations.

www.globalenergyprize.org/en/

International Power Electronics Conference

CIPS 2012, 6 – 8 March 2012, in Nuremberg is the 7th International Conference on Integrated Power Electronics Systems.

Higher power efficiency, density, reliability, and lower volume and cost: How to reach these goals and what solutions are feasible? These topics will be discussed at the 7th CIPS Conference by power electronics experts coming from all over the world.

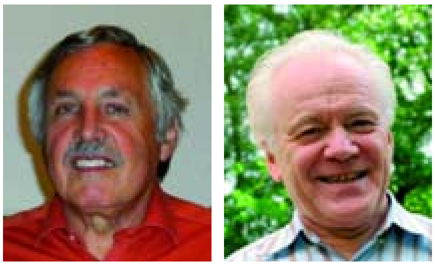

Eckhard Wolfgang, ECPE and Hans-Dieter Silber, University of Bremen Technical Chairs CIPS 2012

Power electronics will remain a key technology in the years to come: Energy saving to protect our climate can be done only by using power electronics systems. Those systems can be found in electronic ballasts for fluorescent and discharge lamps, in efficient induction cookers and variable frequency motor drives. Especially the production of wind and solar energy without power electronics is not possible. Also the e-mobility relies on efficient and reliable power electronics systems for driving and charging batteries.

Higher efficiencies can be gained by applying system integration based on advanced materials and joining as well as on active and passive components.

Due to improved cooling technologies and reduced use of materials, system costs can be reduced and by applying the "building-in reliability" concept the total system reliability will be improved. Computer aided design and test tools are necessary to achieve a "first right" and robust design.

CIPS 2012 is organized by VDE ETG and ECPE and technically co-sponsored by the IEEE PELS and ZVEI. The conference papers undergo a peer review process which allows their introduction to the IEEE Xplore digital data base.

The Technical Program Committee selected 85 out of 105 abstracts. 45 of them will be oral and 28 will be poster presentations. The best poster as well as the best young engineer's presentation will be awarded.

The frame of these presentations is given by three keynote papers and nine invited papers which will provide an overview on the state-of-the-art of the most important topics:

Keynote Papers:

Extreme Efficiency Power Electronics: Johann W. Kolar, ETH Zurich, Switzerland

Reliability of Power Electronics Under Thermal Loading: Patrick McCluskey, University of Maryland, USA

SiC Device and Power Module Technologies for Environmentally Friendly Vehicles: Kimimori Hamada, Toyota Motor Corporation, Japan

Invited papers:

Advanced Cooling for Power Electronics: Sukhvinder Kang, Aavid, USA

Analysis of Innovative Packaging Technologies and Trends for Power Modules: Alexandre Avron, Yole, France

Electromagnetic Modeling of EMI Input Filters: Andreas Muesing, Gecko Research GmbH, Switzerland

On-chip System Integration: Ashraf Lofti, Enpirion Inc. USA

Combined Reliability Testing: An Approach to Ensure Reliability Under Complex Loading Conditions: Olaf Wittler, Fraunhofer IZM, Germany

Integrated High Power Modules: C Mark Johnson, University of Nottingham, UK

SiC and GaN Devices – Competition or Coexistence? Nando Kaminski, University of Bremen, Oliver Hilt, FBI Berlin, Germany

Planar Interconnect Technology for Power Module System Integration Norbert Seliger, University of Applied Sciences Rosenheim, Karl Weidner, Siemens CT, Germany

Reliability of the Planar Skin Interconnect Technology:
Uwe Scheuermann, Semikron, Germany

www.cips-conference.de

Technology Developement Centre in Munich

Fairchild Semiconductor is going to inaugurate the newly formed Technology Development Centre (TDC) in Munich, Dornach in Q1/2012. The TDC is located conveniently in the Einstein Business Centre, well connected by public transport (S-Bahn Riem and U-Bahn Messe) as well as to the Autobahn (Riem). Including all expansion options, the new Fairchild location will be accommodating around 100 people in 1900m2 including a versatile high-voltage characterization and application lab. "The new Fairchild R&D location will represent a hub for innovation for new technologies and products in the high-voltage arena including wide-band gap materials and high-power modules", says Alfred Hesener, Sr. Director of Marketing and Application Engineering Europe.

www.fairchildsemi.com

Carbon Nanotubes Best for 3D Electronics

Researchers at Chalmers University of Technology have demonstrated that two stacked chips can be vertically interconnected with carbon nanotube vias through the chips.
This new method improves possibilities for 3D integration of circuits, one of the most promising approaches for miniaturization and performance promotion of electronics.
Three dimensional integration is a hot field within electronics since it offers a new way to package components densely and thus build tiny, well-functioning units. When stacking chips vertically, the most effective way to interconnect them is with electrical interconnects that go through the chip (instead of being wired together at the edges) – what are known as through-silicon vias.
The industry thus far has primarily used copper for this purpose; however, copper has several disadvantages that can limit the reliability of 3D electronics. Another major issue involves cooling when the chips get hot. The excellent thermal qualities of carbon nanotubes can play a decisive role in this respect.

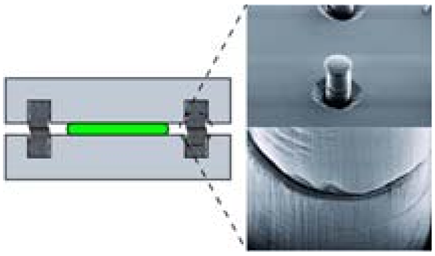

Thus a research team at Chalmers is working with carbon nanotubes as conductive material for through-silicon vias. Carbon nanotubes – or tubes made of graphene whose walls are only one atom thick – are going to be the most reliable of all conductive materials if it is possible to use them on a large scale. This is the opinion of Kjell Jeppsson, a member of the research team. "Potentially, carbon nanotubes have much better properties than copper, both in terms of thermal and electrical conductivity", he says. “Carbon nanotubes are also better suited for use with silicon from a purely mechanical point of view. They expand about the same amount as the surrounding silicon while copper expands more, which results in mechanical tension that can cause the components to break."
The researchers have demonstrated that two chips can be vertically interconnected with carbon nanotubes by through-silicon via interconnects, and that the chips can be bonded. They have also demonstrated that the same method can be used for electrical interconnection between the chip and the package.

www.chalmers.se

German Team Wins European Analog Design Contest

A team of students from RWTH Aachen University in Germany has won the second TI European Analog Design Contest with its project titled "Non-Contact System for Thoracic Activity Monitoring."
The team, made up of Daniel Teichmann, Jerome Foussier and Jing Jia, took first place despite tough competition from 155 teams across Europe. The other winners were:

- Second place: University of Freiburg, Germany, for "Weather in a Box."
- Third place: Warsaw University of Technology, Poland, for "Biofeedback Device."
- Fourth place: University of Lodz, Poland, for "Patient Activity Monitor for Holter Examination."

The Analog Design Contest offers students a chance to work on a design project while using TI’s broad range of high-performance analog ICs. Teams consisting of a minimum of two students can participate with projects using three different TI analog ICs or two analog ICs and a TI processor.
Judging criteria include engineering analysis, originality, quality and creativity in designs featuring TI analog integrated circuits." The top 20 teams automatically progress to the second level of judging and compete for the "Engibous Prize for Innovation in Analog.

www.ti.com/adc

Future Trends for Power Semiconductors

ECPE Workshop Future Trends for Power Semiconductors
26 January (evening) – 27 January 2012,
Zurich, Switzerland

Chairmen: Prof. J.W. Kolar, ETH Zurich
Prof. D. Silber, University Bremen
Prof. L. Lorenz, ECPE e.V.

The ECPE Calendar of Events 2012 is available on the website

www.ecpe.org

Future AC Variable Speed Drive Design

Parker Hannifin’s latest addition to its AC variable speed drives range the AC30V is the first of an entirely new generation of drives products from Parker and has been designed specifically to meet the rigourous demands of industrial pump, fan and general purpose applications.

Initially available in three frame sizes with standard dual mounting options of either IP20 backplate or through-panel mounting, the AC30V will cover the power range 0.75 kW to 18.5 kW (variable torque rating). Fully enclosed IP55 and coldplate mount versions along with extended power capabilities up to 110 kW will be introduced progressively.

Its modular design has enabled Parker to create an AC30 Series which will evolve to include customised variants for complex process or specialised applications. This modularity also reduces the inventory requirements and associated costs for the stockist or end-user alike.

An all new easy to use graphical keypad provides full access to all drive functions simply and intuitively. The clear and easy to read backlit LCD display can present information in any one of ten different languages including simplified Chinese.

With the integrated configuration wizard, it is now possible for users to configure the drive in a matter of minutes without having to be an expert. The wizard guides the user through the setup procedure in a number of simple steps and automatically takes care of the majority of the drives parameters. Once configured, an autotune function ensures the drive is optimised to the motor and drive parameters can then be stored on a standard SD card for backup, or be used to set up other drives.

AC30V has been designed with simplicity in mind, but this doesn’t compromise its functionality. Integrated macros for a range of applications and PLC functionality enable more capable users to create sophisticated control that would previously have required a separate PLC. More flexibililty can be provided by the addition of one of the numerous optional field-fittable I/O cards that are available.

For users with minimal control and diagnostic requirements, the free to download ‘Drive Quicktool‘ software package enables users to configure, monitor and control the drive simply and easily from a laptop computer. Once again the simplicity doesn’t compromise the functionality as the software enables users to connect either directly to the drive or across a LAN network. Automatic detection of the drive’s IP address by the software makes it easier for the user to correctly identify the AC30 drives from other equipment that may be on the same network.

AC30V has been designed for use in even the most arduous of environments. With an extended operating temperature range of 0 to 50 °C, conformal coating to 3C3 as standard, integrated EMC filter to C2 1st environment and integrated DC choke to reduce line harmonics, you can be confident that not only will the AC30V operate in any application, but also that it will not have a negative effect on other electrical systems in the immediate area in accordance with EN61800-3.

With Ethernet communication as standard and integrated user configurable web pages, the AC30V is ready out of the box to fit into many new or existing applications. However, the AC30V can also integrate seamlessly into other industrial networks with the addition of optional communications cards supporting a host of popular fieldbus communications such as Profinet, Profibus, Ethernet IP, Bacnet, EtherCAT, DeviceNet, CANopen and Modbus TCP/IP.

www.parker.com

Digitally Powered

Energy control advances in PFC make going digital simply brilliant.

Cirrus Logic High-Efficiency Digital Power Factor Correction ICs

The Cirrus Logic CS1501/1601 are high-performance active digital power factor correction (PFC) controllers that intelligently solve complex power management challenges. With an industry standard pin out, these ICs offer best-in-class THD, power factor and efficiency across all load conditions, while also reducing the size and number of required external components. A variable on-time/variable frequency algorithm achieves close to unity power factor while spreading the EMI frequency spectrum to reduce requirements for conducted EMI filtering. Cirrus Logic is advancing energy control for PFC solutions to make going digital simply brilliant.

Powerful stuff? To learn more, visit www.cirrus.com/bpspfc and order a free sample.

CIRRUS LOGIC®

Approaches to Optimizing DC-DC Power Design, Without Compromise

By Mark Cieri, Director of Marketing and Dr. Ahmed Abou-Alfotouh, Manager, Systems Architecture Group, Enpirion

Whether for industrial, embedded, telecommunications, enterprise, or storage applications, designers of electronic systems face substantial hardware design challenges when it comes to power management. Challenges include the drive to higher-density form factors with rising bus speeds; increased functionality/storage/processing capacities; shrinking semiconductor geometries; ICs with more power rails; and ever-present pressures toward lowest total cost with fastest time to market — all while facing scarcity in critical hardware development resources.

When selecting point-of-load voltage regulator solutions, designers often assume they will have to compromise in one or more areas, such as targeted efficiency, noise, transient response, thermal management considerations, total cost, solution size, or design complexity. For example, they might feel the need to select a linear versus a switching regulator or a discrete regulator versus an integrated module.

Working with many first-time PowerSoC (power system-on-a-chip) customers, we often find that assumptions about compromises are more like modern-day myths. Very high-density DC-DC PowerSoCs with fully integrated inductors, like those offered by Enpirion, benefit from focused investments in the underlying elements of DC-DC conversion — notably high-frequency semiconductor and magnetics technologies, integrated lead-frame packaging, and comprehensive DC-DC system engineering. As a result, PowerSoCs are ready to tackle a range of IC power management challenges directly, leading to more optimized customer solutions.

For example, higher power efficiency arises from minimizing the sources of power loss. Switching and conduction losses are primarily associated with semiconductor power FETs and the inductor; additional losses are due to device and PCB parasitics. Discrete DC-DC converters often meet efficiency targets by lowering frequencies and using larger off-the-shelf external inductors. The aim is lower losses, but the result is larger current loops and problematic exposed magnetic fields. These designs must contend with higher radiated noise and ripple, often adding to the challenge of PCB design. Efforts to drive discrete DC-DC converters to smaller footprints with higher frequency only add to circuit board noise challenges, generally resulting in prototype iteration.

In contrast, PowerSoCs from Enpirion achieve low-loss, high-frequency operation by the novel implementation of CMOS with LDMOS technology, along with magnetics that are an order of magnitude smaller than discrete converters. High-density PowerSoCs achieve up to 96% efficiency, compared to much larger DC-DC converters, while also suppressing switching noise sources.

This small-but-efficient approach is the result of deliberate innovations implementing fine-line FET technology, which capitalizes on very small transistors to achieve high process Figure Of Merit (i.e., Q*R), along with low-loss magnetics that use proprietary geometries and materials optimized for high-frequency operation. Compact integration of these two key components — together with control, compensation, and high-frequency filters using advanced lead-frame construction — provide especially low parasitics and thermal resistances. The resulting high-density PowerSoC design mitigates undesirable losses, delivering efficient, low-noise, and thermally robust products.

Beyond its three fundamental technology innovation areas, Enpirion focuses heavily on comprehensive DC-DC system engineering, including the design of the power stage and integrating compensation. This effort ensures that customers meet all performance targets while also significantly compressing their required design process and achieving first-pass prototype success. As such, designers enjoy faster time to market without compromise.

Taking a closer look, PowerSoC solutions include pre-selected external components (i.e., no web tools required), completed regulator design, and certified PCB layouts. Behind the scenes, power system engineering focuses on achieving optimized footprint, noise, input/output ripple, load transient and stability attributes. These PowerSoC engineers characterize all subcomponents and perform rigorous system simulations and validation across broad parameters related to silicon, inductor, capacitor, small-signal components, operating conditions, and circuit board layouts. System engineering enables plug-and-play designs that attain performance targets for system noise and time domain with the smallest and fewest components and lowest solution cost.

By contrast, traditional DC-DC converter solutions minimize attributes such as noise and transient response by reducing the frequency, adding more capacitance, and guard banding. Additionally, alternative DC-DC switchers often require secondary input and output filtering; in especially noise-sensitive power rails, they might even use LDOs. These approaches lead to compromises in bill of materials (BOM), PCB area, and efficiency. Their longer and more iterative design processes also sacrifice time to market.

PowerSoCs, as complete engineered IC-level systems, also optimize reliability — with 8 to 10 times improvement versus regulators, which have significantly more external components, especially the inductor. Enpirion's PowerSoC system MTBF (Mean Time Between Failure) is greater than 21,800 years. To ensure PowerSoC reliability, Enpirion manufacturing tests key system functionality, and engineering conducts extensive IC-level JESD qualification.

In addition, PowerSoC systems improve thermal performance, operating reliably over a wide temperature range. The devices minimize internal device power dissipation and efficiently route heat through the low thermal resistance path, namely the integral copper-based lead frame assembly connected to thermal vias. In contrast to commonly accepted practices, this robust PowerSoC design does not require load de-rating, heat sinks, or airflow at industrial-rated temperatures of 85°C.

In summary, through innovative and focused engineering, PowerSoCs challenge traditional DC-DC power design paradigms. Enpirion has developed key intellectual property in the areas of high-frequency IC technology, low-loss magnetics, and advanced power packaging that enables very small and high-density DC-DC PowerSoC solutions. Electronic hardware designers can achieve high efficiency, low noise, high reliability, ease of design, and lowest total cost for a variety of applications — all at the same time. In other words: optimized power management without compromise.

www.enpirion.com

ELECTRONICS INDUSTRY DIGEST

By Aubrey Dunford, Europartners

GENERAL

Booming shipments of ultrabooks during the next four years will shake up various semiconductor markets, boosting the prospects for sensors as well as power and analog semiconductors, but decreasing the market opportunity for upgrade memory modules, so IHS iSuppli. Global ultrabook shipments are expected to soar to 136.5 million units in 2015, up from less than 1 million in 2011.

SEMICONDUCTORS

As many semiconductor vendors announced relatively weak sales for the third quarter of 2011, and preannounced poor guidance for the fourth quarter, the anticipated inventory correction is well under way, so Gartner. This process will continue to dampen sales prospects for at least the remainder of the year before sequential growth can return in 2012.

Global semiconductor revenue in 2011 now is expected to rise by 1.2 percent compared to 2010, so IHS iSuppli. This is down from the previous IHS forecast of 2.9 percent issued in September. IHS forecasts 2012 semiconductor revenue growth will amount to an anemic 3.2 percent. A return to stronger growth will not begin until 2013.

40 years ago, Intel introduced the world's first commercially available microprocessor – the Intel 4004 – triggering the start of the digital revolution. Compared to the Intel 4004, today's second-generation Intel Core processors are more than 350,000 times the performance and each transistor uses about 5,000 times less energy.

Globalfoundries has postponed its plan to start building the Gulf's first microprocessor-fabrication plant in Abu Dhabi next year.

The company, which is 91 per cent owned by Abu Dhabi's Advanced Technology Investment Company (ATIC), will not start construction of the facility next year because of the uncertain global economic outlook, so local media reports.

The ENIAC Joint Undertaking announced that the project "Nanoelectronics for an Energy Efficient Electrical Car (E3Car)" received its 2011 innovation award, demonstrating 35 percent energy savings, lower costs, improved reliability and shorter time to market by introducing innovations at component and sub-system level, some of which are being adopted in real-life applications as early as in 2012. With a combined R&D budget of € 180 M and more than 100 participants from the whole value-creation chain, these projects shall generate knowledge and product prototypes substantiating the European claim for electronic leadership in the rapidly growing electro-mobility sector. The consortium is coordinated by Infineon Technologies.

OPTOELECTRONICS

Innovation Network Corporation of Japan (INCJ), Hitachi, Sony and Toshiba have signed definitive agreements to integrate their small- and medium-sized display businesses in a new company to be established and operated by INCJ, which is planned to be named Japan Display. INCJ.

Based on panel makers' shipment targets in Q411, 209 million LCD TV panels will be shipped in 2011, 5 percent less than the 220.8 million shipped during 2010. This would make 2011 the first year that LCD TV panel shipments decreased.

PASSIVE COMPONENTS

Germany's PCB revenues for August reached the third highest level of the last 10 years, so the ZVEI. Sequentially, August revenues were up 2 percent, while year-to-date figure improved by 14 percent over the same period last year.

OTHER COMPONENTS

Agilent announced that Ron Nersesian has been appointed executive vice president and chief operating officer. He has been president of Agilent's largest business, the Electronic Measurement Group (EMG), since 2009.

DISTRIBUTION

European distribution bookings in Q311 declined by 18.4 percent compared to the previous quarter and by 22.7 percent when compared to the same period in the previous year, so the IDEA (International Distribution of Electronics Association). Sector specific bookings changes in Q311 compared to the same period in 2010 were: semiconductors declined by 27.5 percent; passives declined by 20.6 percent; and electro-mechs and other components declined by 5.2 percent. European distribution billings in Q311 declined by 11.8 percent, when compared to the previous quarter and by 2.4 percent compared to Q310.
Avnet has agreed to purchase the French company DE2, to strengthen its Avnet Embedded business unit in EMEA.

In the first half Electrocomponents revenue grew by 11 percent year on year at £ 626.5 M, the International business grew by 14 percent and the UK by 5 percent. Profit before tax grew by 17.6 percent at £ 59.4 M. eCommerce revenue grew by 26 percent and represents 54 percent of group sales at the exit of the half year.

This is the comprehensive power related extract from the « Electronics Industry Digest », the successor of The Lennox Report. For a full subscription of the report contact:

eid@europartners.eu.com
or by fax 44/1494 563503.

www.europartners.eu.com

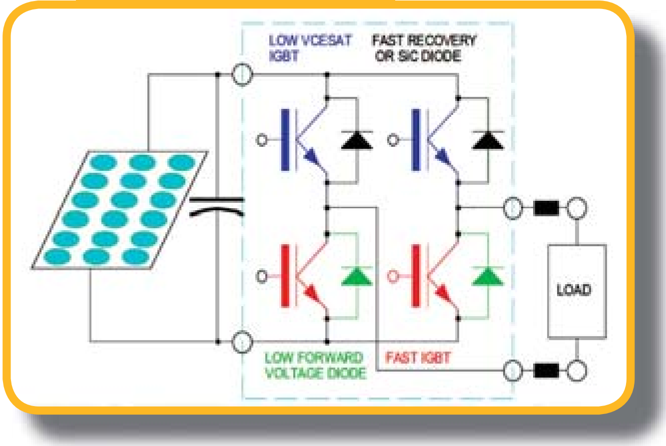

LOW VCESAT IGBT
FAST RECOVERY OR SiC DIODE
LOAD
LOW FORWARD VOLTAGE DIODE
FAST IGBT

New Power Distributions Detailed at Darnell's DC Building Power Asia

By Linnea Brush, Senior Research Analyst, Darnell

The latest developments in dc building power were highlighted at Darnell's DC Building Power Asia conference, held December 12-13, 2011, in Taipei. This market is projected to grow significantly over the next several years, and the conference focused on where those opportunities are. Several trends are driving growth, including the smart grid, dc microgrids, LED lighting, integrated power management and energy storage, and data center/telecom powering requirements.

Several papers focused on how dc powering can address the challenges faced by data centers, including "Modular High-Efficiency Non-Isolated 380Vdc Power System for Data Center," "New Plug and Socket Outlet for 400Vdc, 10A," and "Smart DC Power Supply System for Telecom Industry and Data Centers." These systems are being implemented now, and were discussed in detail by speakers from Delta Electronics, Fujitsu, and Chung Hsin Electric Manufacturing Group.

For example, Delta's approach for improving energy use in data center infrastructure includes commercializing a 380Vdc power system that incorporates environmental monitoring software and data center precision cooling. Such a system can lead to higher efficiency, reliability and power density, as well as lower cost, better power quality and "excellent" phase balance. It also makes it easier to integrate with renewable energy sources, such as photovoltaics, wind power and fuel cells.

A project currently being implemented was described in the paper, "Green IT Project in Korea – 380Vdc Distribution System Design and Analysis." In Korea, research on green IT technology for residential and commercial buildings is underway, partially funded by the Korean Ministry of Knowledge and Economy. The project is focused on the realization of dc power distribution systems and energy management systems, which is conducted by Seoul National University and Korea Electronics Technology Institute, respectively. This research is mainly focused on the application of dc technologies in residential and commercial buildings.

In the first year, dc distribution system configurations (ac and dc, distributed dc, transmitted dc), and system parameters such as distribution voltage with a view of efficiency, safety, cost, compatibility, were implemented. To observe the feasibility of a dc system, loads were classified based on their type and power conversion stages. In 2011, dc appliances such as refrigerators, TVs, PCs, LED lamps, irons and air-conditioners were developed. Research on dc technologies such as inrush current protection, dc EMI filters, dc switches, and circuit breakers is also being conducted. The experimental results showed increased efficiency of the entire system, utilizing a high-efficiency ac-dc power supply developed during the past year.

In addition to advances in dc power for data centers, new advances in solid-state lighting (SSL) are expected to drive the dc power market over the next several years. Used in large high-definition signs, architectural lighting, stadiums, billboards and other applications, modern LEDs represent the latest lighting devices based on dc power. "Dramatic" improvements in commercially available LED performance, significant cost reduction, government regulations, and energy savings could also help drive the LED replacement market.

At DC Building Power Asia, Germany's Osram AG described new LED drive approaches that are designed to optimize solid-state lighting performance and reduce cost in buildings with dc power distribution architectures. In both cases, 380/400Vdc power distribution was identified as an optimal power source. Although the efficiency of the linear driver is lower than a corresponding switch-mode driver, the linear driver can still achieve 85% or greater efficiency if the input dc power bus is relatively stable. With a well-regulated dc power bus, the efficiency is 10% lower compared with a switch-mode solution, and the cost is over 60% lower, dramatically reducing the overall cost of the luminaries.

During the plenary session, ITRI discussed "LED Lighting, Now and Future." Because the cost of LED lighting is a key factor slowing the adoption of this technology, high-voltage dc power is a key way to reduce the cost of the three highest-cost elements in an LED lighting system: the LEDs, the heat sink and the driver.

A cost-effective solution is to use a compact LED light-engine in which the dc-dc driver IC and LED chips are bonded on the same substrate. Operation directly from 380Vdc input power reduces the number of components in the driver circuit, substantially lowering the cost. In addition, by using the latest high-voltage LEDs, a higher operating efficiency can be achieved, reducing heat generation and lowering the cost of the needed heat sink.

DC microgrids got a lot of attention at DC Building Asia, as well. In the US, microgrid deployment is driven by several factors, including an uneven power distribution where new technologies can offer greater value to both end-use customers and utilities. Utilities have historically been opposed to microgrids because of their wish to maintain control over grid operations and potential safety concerns. But recently the IEEE published a standard to ensure "safe-islanding" for a microgrid to continue operation and protect distribution line workers in the even of disruption in the larger grid.

The opening presentation at DC Building Asia detailed a master plan for the implementation of smart grid technologies in Taiwan by 2030 by the Chair of the National Energy Project – Smart Grid and AMI Division, National Science Council. Among the topics presented were "cellular smart grids," smart home energy systems and the use of advanced distribution automation technologies to enable the absorption of high levels of distributed generation resources.

A "Multi-Microgrid" calls for a series of arbitrary microgrid elements that could be integrated or separated like building blocks to modify the size and structure of the microgrid in real time in response to changing conditions in renewable energy resources and energy demand. This concept is expected to support the development of Cellular Smart Grids.

Other topics addressed included energy storage solutions, such as "Integrated Power Management and Energy Storage," presented by ZBB Energy Storage. ZBB discussed an integrated management platform that supports the integration of any combination of generating sources, including having the grid as a two-way input. By adding energy storage, the platform creates an expandable power plant system that optimizes the supply of each energy source. The modular architecture allows expansion, including the use of non-interrupted dc power distribution for emerging classes of dc voltage devices, such as variable frequency drives, LEDs, elevators and system controls. Power can be regenerated directly back to the dc bus, delivering a more efficient use and firmer supply of renewables.

The conference concluded with a tour of a fuel cell and smart meter laboratory at Chung-Hsin Electric & Machinery Mfg. Corp. (CHEM). CHEM is a member of the Taiwan Smart Grid Association, focusing on microgrids, and their objective is to develop and demonstrate a smart DC microgrid with renewable energy power sources synchronized to the grid for data center and telecom applications. CHEM's "Smart DC Building" model includes a bi-directional dc-ac inverter taking grid power to feed a high-voltage 380-430Vdc bus; along with a bi-directional dc-dc converter using renewable energy power to feed low-voltage 24/48Vdc loads.

Although still in the early stages, dc building power is slowly emerging as a viable and cost-effective alternative to ac powering. The power requirements are not trivial, however, and these challenges present multiple commercial opportunities for power supply companies.

DC Building Power Asia:

http://dcbuildingpowerasia.darnell.com/

1mW Isolated DC/DC Converter

Extreme low current consumption of the microcontroller

Nowadays we're living in an era of metering and sensing. More physical factors are measured and collected then ever before, data is linked up and by the use of the internet sensor data can be looked up from every place of the world. The tendency is to replace bulky mechanical meters and sensors by electrical ones. They offer a lot of more flexibility and possibilities but they also need always some kind of electrical power supply. Fortunately only little power in the range of 1..100mW is needed for most of theses applications.

By Milan Marjanovic & Matthias Ulmann, Texas Instruments

Even better when the needed power is so small, that maybe the data lines of the sensor bus network (RS485 e.g.) can be used to supply the sensor and its electronic. In this case it must be assured to limit the input current and the overall power to avoid a malfunction or damaging of the network, as this operation mode was never intended for most sensor networks. In the following an isolated 1mW DC/DC converter is shown, which uses amongst other things an excessively low-current drawing PWM generator someone wouldn't think first.

Requirements

The tough specifications are shown in the table below. It's easy to see, that with a traditional approach these requirements can not or hardly be satisfied.

Factor	Min.	Max.
Input Voltage [V]	3.1	3.4
Maximum Input Current [mA]	-	1.1
Output Voltage [V]	3.1	3.1
Output Current [mA]	-	0.3
Output Voltage Ripple [mV_{pp}]		5
Isolation Voltage [V_{RMS}]	500	
Load Step	-	2mA for 10ms @ 10Hz

Table 1: Requirements

The three main challenges were identified:

- A very low input voltage and a limited input power of 3.4mW maximum
- The absolute minimum efficiency of the whole converter has to be 27% or better
- A load step of 180% of the maximum allowed input power

To achieve the needed efficiency, all losses of the converter and its circuitry have to be as small as possible. Therefore also a low power PWM controller is needed. Different solutions for generating a PWM signal are known and were compared to each other.

Topology/ Technology	Comment	Benefits	Drawbacks
Flyback	Analog current mode flyback controller	Simple	High startup voltage needed High operating current
Fly-Buck™	Analog current mode buck controller	Simple	High operating current
"Analog" Push-Pull	Analog current/voltage mode push-pull controller	Simple	High startup voltage needed High operating current
"CMOS" Push-Pull	Free running push-pull or full bridge topology	Simple	High operating current
"Digital" Push-Pull	Push-pull topology driven by a small microcontroller	Flexibility	Complexity

Table 2: Topology/ Technology

All solutions except the Fly-Buck™, "CMOS" and "Digital" push-pull need a high start up voltage of >4V and therefore won't work in this application. As the input current has to be limited to 1.1mA, the voltage on the bulk capacitor which supplies the primary side of the push-pull, drops during a load step. Therefore also the voltage on the PWM generator drops and the circuit has to works still properly.

PWM Generator

To generate the PWM signal, also circuits with operational amplifiers and integrated timers like NE555 were tested, but the power consumption was unacceptable. As any low voltage CMOS device or low power microcontroller can be used, both approaches were tested and the microcontroller solution was clearly ahead in respect of power consumption. The CMOS generator needed about 3.5mW and the microcontroller solution with MSP430G2132 only 180µW.
Both devices were supplied by a 1.8V linear regulator TPS71501 with very low power consumption (5µA) to ensure a proper working condition even when the input voltage drops. The low supply voltage reduces also the overall power consumption of the microcontroller. To reduce the losses on the LDO further, a TPS78xx with only 500nA current consumption can be used.

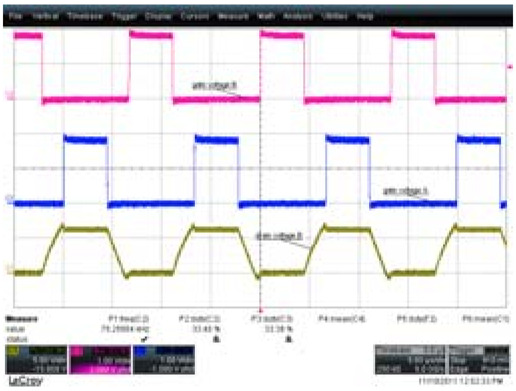

Figure 1: Both PWM signals as well as the drain-source voltage of one push-pull MOSTFET

To keep the voltage regulation simple, the PWM generator works with a fixed duty cycle of 33% on each output and drives the push-pull transformer in open loop at 78kHz. A linear regulator on the output of the push-pull regulates the output voltage for powering the sensor. All microcontrollers need some kind of programming to work as desired. In this case the routine is pretty small and consists of only a few lines of source code. After startup, the peripherals and the main clock are initialized. Then Timer A is set to generate two PWM signals which are shifted 180 degree to each other. The last step is to set the microcontroller in sleep mode LPM0, which reduces the current consumption tremendous. In this mode the CPU and main clock are switched off, but the timer is still running, which is enough for generating the PWM signals for the push-pull.

Programmable Integrated DC-DCs Deliver Big Power and Small Size

10A and 20A Output with Built-in MOSFET's and Digital Control
Advanced Power Management with No Extra Components or Cost

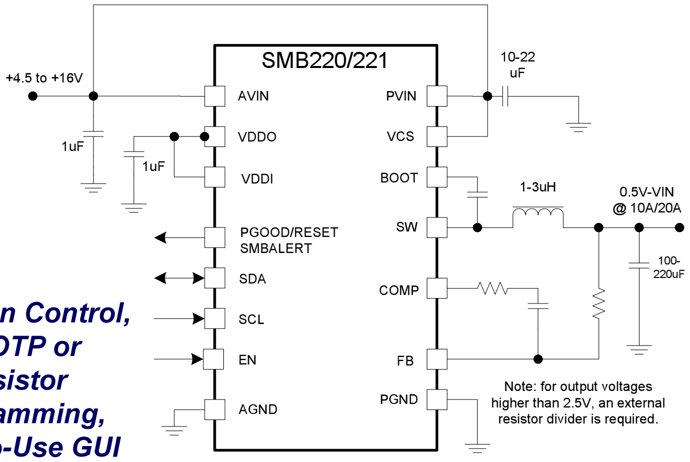

Note: for output voltages higher than 2.5V, an external resistor divider is required.

I^{2}C or Pin Control, NV OTP or Resistor Programming, Easy-to-Use GUI

Features

- Integrated MOSFETs up to 10A/20A output
- 1% Output accuracy
- Digitally Programmable with Non-Volatile OTP Configuration or External Resistors
  - Static/dynamic output voltage/margining
  - Softstart timing/slew rate
  - RESET/PGOOD behavior
- True Current-Mode PWM Control
- Built-in Safety and Protection
  - Cycle-by-cycle current limit
  - Over-temperature protection
- Tiny 5mm x 6mm QFN Package

Applications

- Server, Notebook and Tablet Computing
- Enterprise Switches/Telecom Routers
- POL Power Modules
- Digital/IP Set-Top-Box/DTV/Smart TV
- Storage Equipment and Disk Drives

Efficiency with +12V Input

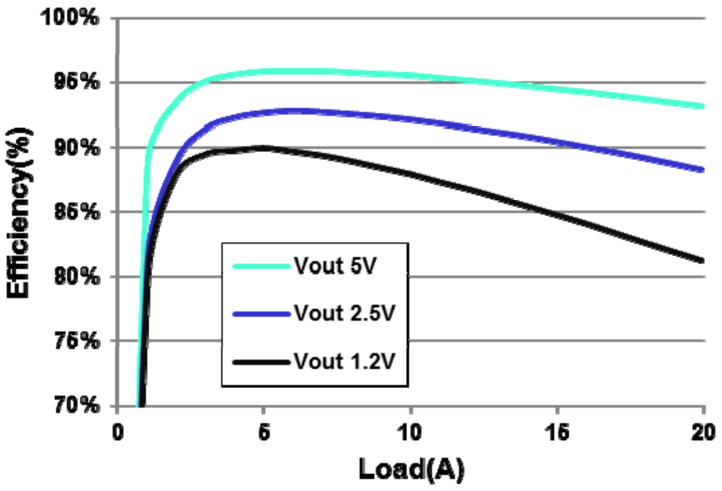

Fewest Components Smallest Footprint

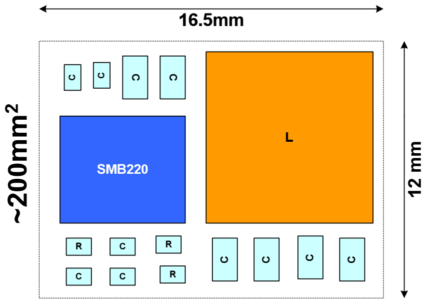

Summit Programmable DC-DC Family

	SMB109/8/6	SMB206/7/8/A	SMB209/10/A	SMB211	SMB220/1
Input Voltage Range (V)	4.5 to 28	4.5 to 16	4.5 to 16	4.5 to 16	4.5 to 16
# of Outputs	2/3/4/8	2	1	1	1
Output Current (A)	>20	1/2/3	4/6	>20	10/20
Switching Frequency (kHz)	300-1200	500/1000	500/1000	250-1000	250-1000
Output Voltage Range (V)	0.5-VIN (Prog)	0.8-VIN (Prog)	0.8-VIN (Prog)	0.5-VIN (Prog)	0.5-VIN (Prog)
Internal/External FETs	External	Internal	Internal	External	Internal
Output Voltage, Seq., Softstart, OCP	Prog	Prog	Prog	Prog	Prog
Output UV/OV Monitor	Prog	√	√	Prog	Prog
RESET/POWER GOOD Output	√	√	√	√	√
I2C/SMBus Interface	√	√	√	√	√
Packages	7x7 QFN-56 5x5 QFN-32	3x3 QFN-20 TSSOP-24	3x3 QFN-20 TSSOP-24	3x3 QFN-20	5x6 QFN-28

For more information see:
www.summitmicro.com/SMB220
www.summitmicro.com/MobileGreen

MobileGreen™ TECHNOLOGIES

SUMMIT MICROELECTRONICS

Programmable Power for a Green Planet™

Of course, the microcontroller can be used for other purposes as well as the PWM generation needs no CPU time and is working autonomous.

Figure 1 shows both PWM signals as well as the drain-source voltage of one push-pull mosfet. The dead time was adjusted to achieve zero current switching, which boosts efficiency.

Component Selection

Primarily the whole circuit has to work at the low input voltage of 3.1V. The PWM modulator with a MSP430 microcontroller or even with a CMOS device fulfills these requirements. It must be also taken care on the gate threshold voltage of the mosfets used to drive the push-pull transformer. A logic level FET like BSS138 with a maximum threshold of 1.5V is appropriate.

Furthermore a very low forward voltage drop of the rectification diodes on the secondary side and low leakage current for all capacitors is needed. As the leakage current can be a problem with electrolytic or tantalum capacitors, only ceramic capacitors are applied.

To fulfill the load step requirement, buffer capacitors on the primary as well as on the secondary side are needed. According to the requirement, the calculations result in a total of 18µF on the input of the converter. To cover all tolerances and deviations, 2x 22µF X7R ceramic capacitors are placed in each case.

For charging this high capacitance on the input, a simple current limiter is added. It limits not only the input current during normal operation to approximately 1mA, but works also as an inrush current limiter when the board is attached to the sensor bus network for the first time and as an overload protection. Due to temperature dependencies the accuracy of this circuit is not that much precise, but it is small and reliable.

The push-pull transformer was custom-made by Wurth Electronics (part number 760390004) and has a total primary inductance of 3.3mH. The turns ratio is 1:1.5 to achieve a voltage on the output which is always higher than the input voltage.

The output voltage of the push-pull is buffered by the capacitors mentioned above. Because this voltage is not constant as the converter is working with a fixed duty cycle at a variable input voltage, an LDO generates a precise voltage of 3.1V. To fulfill the requirements according ripple (max. 5mV) and low noise, a linear regulator TPS71501 with a very good PSRR up to 10MHz is used.

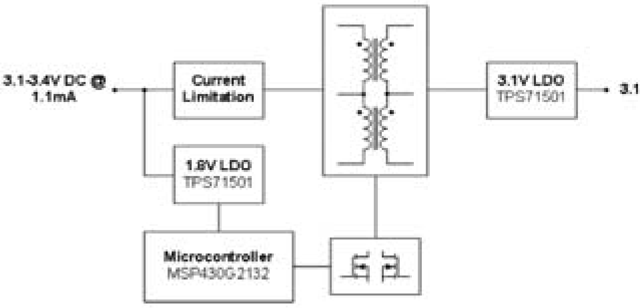

Figure 2: Block diagram of the complete converter

Figure 3: Photo of the complete converter

The block diagram and a photo of the complete converter are shown in Figure 2 and 3. Although the power level is very little, extensive electronic circuitry is needed.

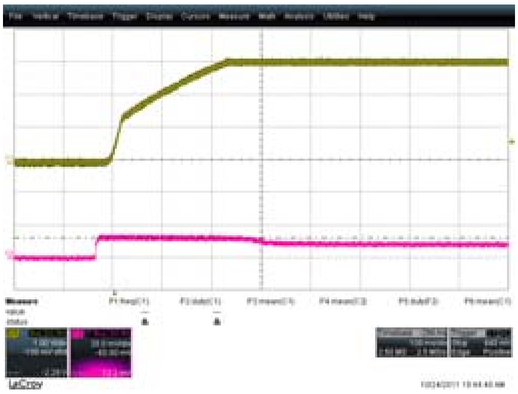

Figure 4: input and output voltage during startup of the converter

Measurements

The input and output voltage during startup of the converter is shown in Figure 4. The voltage is ramping up cleanly within 300ms with no load attached to the output.

To measure the efficiency, the input and output current as well the voltage have to be measured precise. To measure the low currents, a 10 Ohm resistor (1% tolerance) was put in line of the input and output to measure the voltage drop on the resistor. Without any load attached, the system draws approximately 270µA at 3.1V (837µW) and approx. 290µA at 3.4V (986µW) input voltage.

Efficiency at 300ìA load with 3.1V output voltage (930ìW load):

Input Voltage	Input Current	Efficiency
3.1V	720µA	41.6%
3.4V	740µA	37.0%

Efficiency at 300ìA load + 2mA load for 10ms @ 10 Hz (470ìA avg.) with 3.1V output voltage:

Input Voltage	Input Current	Efficiency
3.1V	910µA	51.6%
3.4V	930µA	46.1%

Table 3: Efficiency at 300ìA load

Conclusion

With a microcontroller instead of an analog PWM modulator, a small and reliable power supply with galvanic isolation for sensor applications was developed. For its power level of about 1mW, the peak efficiency of more than 50% is remarkable. This is mainly enabled due to the extreme low current consumption of the microcontroller, which generates the PWM signals for driving the push-pull stage. The whole circuit was built and tested, all data (schematic, layout, bill of material, software) is available on TIs PowerLab™ Reference Design Library (http://www.ti.com/powerlab) with PMP7022 as reference.

References

For more information on the used parts and technologies described here please visit http://www.ti.com and read the corresponding datasheets.

www.ti.com

Smart and Flexible 2.5A Li+ Charger, Tiny Solution for Big Batteries

High-Efficiency, Programmable Flexibility, Universal USB/AC/DC Inputs & Robust Safety Features Deliver a Complete, Cost-Effective Solution

Fastest, Safest and Most Flexible Charging Solution

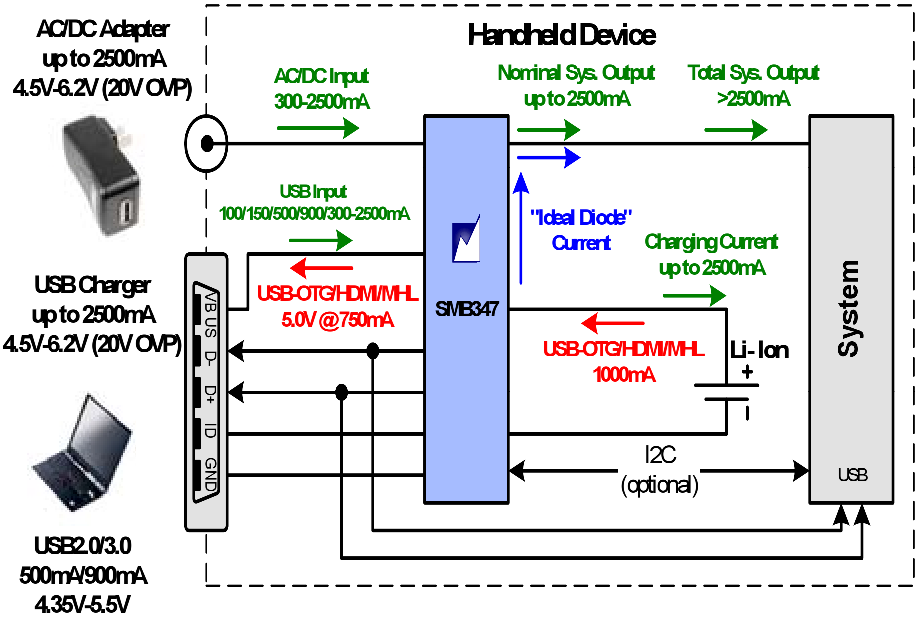

SMB347 Features

- Dual Inputs - AC/DC/USB2.0/3.0
- Dual Output CurrentPath™ for low/dead battery with 'ideal diode'
- +3.6V to +6.2V Input (+20V OVP)
- USB BC1.1/1.2 Source Detection
- Programmable Input Limit to 2.5A
- Automatic Input Limit Detection*
- Programmable Charge Current to 2.5A
- Integrated 5V USB-OTG Boost Output
- TurboCharge™* for 40% Faster Charging
- Robust Safety: JEITA/IEEE1725 Support
    - Over-Current/Over-Voltage
    - Thermal Monitor
    - Input Detection and Fault Status
- <10uA standby current
- I²C Programmable (Volatile and Non-Volatile)
- 2.5mm x 3.0mm CSP Packaging

** Patented*

Programmable Switch-Mode Battery Charger Family

	SMB347/346	SMB328A/B	SMB137B/136	SMB329B	SMB338P
Input Voltage Range (OVP)	4.0 to 6.2 (20)	4.0 to 6.3 (20)	4.0 to 6.0 (18)	4.0 to 6.2 (20)	4.0 to 6.2 (18)
# of Inputs/Outputs	2/2	1/1	2/2, 1/2	1/1	1/1
Maximum Charge Current (mA)	2500/1250	1200	1500	1150	1250
Battery Thermal Protection	HW JEITA	HW JEITA	SW JEITA	√	
USB Charging Spec	rev 1.1/1.2		rev 1.0	rev 1.0	
Package (mm)	3.0x2.5 CSP	2.2x2.0 CSP	3.0x2.5 CSP	2.2x1.9 CSP 4x4 QFN	2.2x1.9 CSP

>90% System Efficiency

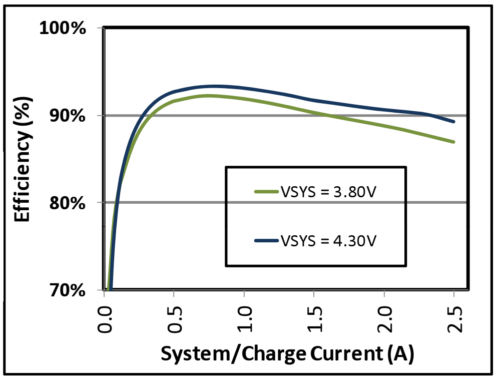

For more information see:
www.summitmicro.com/SMB347

SUMMIT
MICROELECTRONICS, Inc.
*"Programmable Power for a **Green** Planet™"*

Keep Cool

Liquid Cooling Meets Advanced Requirements of Power Electronics

So far nobody has succeeded in designing an electronic component with a 100% efficiency, so power that is lost during operation is transformed into heat. In order to avoid exceeding the acceptable temperature limit and subsequent destruction of the component, this heat needs to be removed as effectively as possible.

By Rainer Selisko, Thermal Management Sales & Technical Support,
Mersen Germany and Austria

Advanced power electronics are gradually reaching the limits of air cooling solutions. The trend to attain higher and higher power in more compact sizes requires efficient solutions, which can be achieved by liquid cooling. Possible misgivings based on the presence of water in a touchy electric environment are no longer an issue today; up-to-date technologies like vacuum brazing have dispelled these concerns. Today's market offers users of power semiconductors a variety of technologies to choose from. However, the pros and cons for the individual application demand careful evaluation. Not only thermal performance, but also electrochemical, mechanic and hydraulic challenges have to be taken into consideration when designing the technologically ideal cooling plate.

Entry Level Technology for Liquid Cooling

Cooling plates with embedded pipe meanders are the so-called entry level technology for liquid cooling. S-shape copper tubes or, in exceptional cases, stainless steel tubes are mounted into an aluminum base plate. The most common version is a serpentine copper tube glued into a one-sided pre-machined base plate. The pipe bends may be positioned inside or outside the aluminum plate. These pipes are squeezed and milled on the surface to reach an even contact plane. The alternative is to insert the copper tubes into channels drilled centered and longitudinal into the plate, which requires brazing the connections after assembly. The thermal contact is achieved by expanding the tubes, for instance, by pulling a mandrel through them.

Cooling plates equipped with copper tubes can be manufactured at a competitive price and are used for low- to medium-high thermal requirements. Copper is an excellent heat conductor which also tolerates „contaminated" cooling liquids. The thermal resistance between the tube and the aluminum plate makes the cooling effect on the complete contact surface of the cooling element slightly inhomogeneous. When positioning the electronic components onto the cooling plate, the limited bending radius of the tubes has to be observed and this does not always support a space-saving layout. Although tubes made of stainless steel resist corrosion and aggressive substances pretty well, they do have a low thermal conductivity and are more difficult to work with. The meander can only be mounted into the aluminum plates from one side, otherwise the end turns would have to be welded for centered tubes. A special cooling plate design is manufactured by utilizing stainless steel tubes embedded in cast aluminum. Cast aluminum, however, has a slightly lower heat conductivity compared to extruded aluminum, and requires its own casting mold, depending on size.

Liquid Cooling Plates Utilizing Aluminum Profiles

If aluminum can be used in direct contact with the cooling liquid, a pure aluminum cooling plate sports considerable advantages. The heat transfer between the tube and the plate is eliminated, enabling the entire assembly to become lighter in weight. The basis is a profile with longitudinal drilled holes. This profile is then equipped with cross drillings to redirect the coolant flow, this requires plugging the unused openings. An alternative is to machine the direction change channels at the plate end and to close them with a welded-on cover. To reach better flow characteristics in the straight channels, turbulators are inserted in some cases. The biggest advantage is a simple, cost-effective design. Obviously, on the other hand, some restrictions in the positioning of water channels, hot spots and mounting holes are inevitable. Design-based sharp corners in the channels may also cause a high pressure drop in the cooling circuit.

Milled Aluminum Cooling Plates

To optimize the cooling circuit according to the components' positions and thermal requirements, designs equipped with milled water channels are an attractive solution. The cooling liquid can be directed exactly under the hot spots of the power semiconductors and around their mounting holes. A high flexibility is reached for the positioning of various components on one cooling plate, which at the same time serves as a support for the electronic elements. An exact cross-section for the desired coolant flow can be dimensioned, thus achieving an optimized liquid velocity and a minimum pressure drop. Correct designing of the channels creates optimized turbulences in the cooling liquid which in turn achieve the best possible heat transfer. Machined base plates must of course be closed with a cover; the simplest solution being to bolt it with a gasket. However, this entails a certain risk of leakage which increases with larger plates. A solid and tight joint can be achieved by welding the lid to the base; by classic gas-shielded, friction or laser welding.

Vacuum Brazing is First Choice

A completely homogeneous connection between the milled base plate and the cover plate can only be achieved through vacuum brazing. This technology combines all the advantages of the above-mentioned thermal and hydraulic properties with other merits such as an optimized heat transfer to both sides of the coolplate, extreme mechanical strength, absolute tightness and extremely long life. An aluminum plate with machined cooling channels is used as a base. The cover consists of two parts: the brazing sheet and the actual cover plate. The thin aluminum brazing sheet is plated on both sides with an aluminum alloy with a low melting point, positioned between the base plate and the cover. The entire stack is then fixed with a clamping device and heated in a vacuum furnace. The temperature-time curve during the process demands a tight control in order to reach a completely homogeneous heat diffusion and a temperature between 580 and 600°C in the cooling plate. During the process the liquefied plating of the brazing sheet creates a completely homogeneous bond with the adjacent aluminum parts. Many years of development and experience in this field of technology enable Mersen to master this sensible brazing process to absolute perfection.

Cooling plates manufactured in a vacuum brazing process show an excellent heat transfer on both sides of the cooling circuit, making them the perfect choice for double-sided placement. Because of the consistent connection of each wall between the channels with the cover, complete sealing is achieved, not only to the exterior, but also between the individual channels. The resulting excellent high-pressure resistance gives certitude that the coolplate will not buckle when subjected to hydraulic shocks in the cooling circuit which could lead to destruction of the electronic components. Vacuum brazing technology can also be used to manufacture multi-layer coolplates in a single brazing run. Even very complex cooling circuits, for instance countercurrent circuits for a more homogeneous temperature distribution below one or more components, can be designed.

Vacuum-Brazed Cooling Plates for Standard Applications

Based on experience with a multitude of customer-oriented technical solutions, Mersen is in the process of developing a range of vacuum-brazed cooling plates for standard applications. The new standard product line will combine all the advantages of high-tech coolers for small and medium quantities at attractive prices. The first version that will be shortly available off the shelf is multifunctional and can be used for two IGBTs measuring 140 mm x 190 mm or three IGBTs 130 mm x 140 mm. All mounting holes are predrilled and G3/8 thread water connections are provided. The cooling circuit has been designed for countercurrent, achieving an excellent temperature distribution on the entire contact surface. The Rth for an IGBT 140 mm x 190 mm (heat transfer area 102 mm x 190 mm) reaches 14 to 4.5 K/kW, depending on the cooling liquid composition and flow rate.

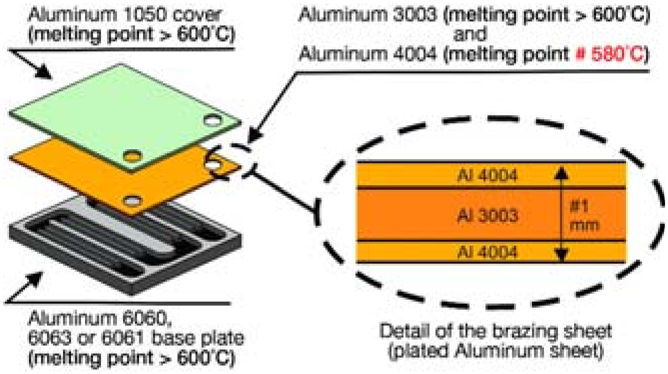

Figure 1: Thermal, hydraulic and mechanic optimum: Design of a water cooling plate manufactured with Mersen vacuum brazing technology

Figure 2: The new generation of standardized water cooling plates for IGBTs offers an affordable high-tech cooling solution, even in small quantities

Here is an application example for two IGBTs 140 mm x 190 mm, both emitting a power loss of 1000 W: using water with an inlet temperature of 40°C and a flow rate of 10 l/min, the plate surface only reaches a maximum temperature of 46°C on the hottest spot. The temperature difference underneath the semiconductors is less than 2°C, the pressure loss in the cooling circuit stays below 400 mBar.

www.mersen.com

First Principle Optimization of Power Module Baseplate

Simulation results are found in good agreement with data out of experiments

One of the primary concerns in the design of power modules is the base plate shape. It plays a vital role in the thermal and mechanical stability of the complete module. This paper deals with the generic optimization scheme for base plate shape using finite element method (e.g. ANSYS). Soldering, mounting and operation conditions are considered in the simulation. Stress analysis is performed to observe the influence of the thermal and mechanical factors on the reliability of individual components. An optimized base plate with adequate technical requirements for individual components was designed using simulations and further verified by experiments.

By Ivonne Benzler, Indrajit Paul and Frank Broermann, Infineon Technologies AG

Power modules are key components for clean and efficient technologies in the domain of renewable energies, electromobility and industrial applications. Finite element analysis is widely used for the prediction of resulting base plate shape in power electronics [1], [2]. The main issue involved is the bimetallic effect triggered by thermal variations during soldering process and during operation. Due to this effect, high level of residual stress remained in the module, increasing risks in silicon chips and ceramic DCB breaks by mounting operations. In this paper, a methodology to counter these effects is presented. The methodology used herein highlights how preformed baseplates, thermal bending effects and the utilization of FEA analysis including parameters of soldering processes can be used to achieve the optimal baseplate shape of a specific power module, so that requirements in terms of residual stress, high yield and high reliability for the mounting and operation conditions can be fulfilled.

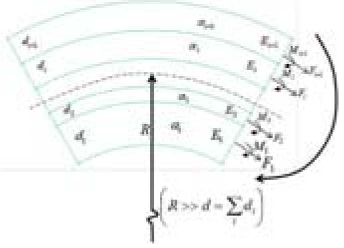

Figure 1a: Bimetallic effect

Force balance:

$$\sum_{i=1}^{N} F_i = 0$$

Moment balance:

$$\sum_{i=1}^{N} M_i + \sum_{i=1}^{N} F_i\left(\sum_{j=1}^{i} d_j + \frac{d_i}{2}\right) = M_{ext}$$

Tangential strain balance:

$$\alpha_i \Delta T_i + \frac{F_i}{E_i d_i} + \frac{d_i}{2R} = \alpha_{i+1} \Delta T_{i+1} + \frac{F_{i+1}}{E_{i+1} d_{i+1}} - \frac{d_{i+1}}{2R}$$

Moment equation:

$$M_i = \frac{E_i I_i}{R}$$

Figure 1b: Thermal bending equations

Theory

When materials with different CTE (Coefficient of Thermal Expansion) values are assembled together through soldering processes and submitted to significant temperature changes, thermal bending associated with a certain radius of curvature of a structure with several layers occurs like shown in Figure 1a. Analytical derivation based on multilayer beam assumption is depicted in Figure 1b. [3]. In this formulation, di, Ii, ?i , Ei, Fi and Mi are the thickness, the second moment of area, the coefficient of thermal expansion, the Young modulus, the tensile force and the moment inside layer i respectively. Mext is the external moment due to the mounting operation and Ti is the temperature of layer i. The radius of curvature of the whole assembly R can then be extracted out of this equation system for a change in temperature between Ti and Ti+1. This provides a simplified method to estimate the radius of curvature for the baseplate.

Optimization methodology

In order to process a flat baseplate, the utilization of the bimetallic effect – well-known as an assembly issue in the electronic industry - is proposed to come over the final bending effects. The starting point of the process optimization consists in stamping the baseplate with a radius of curvature R1 before the soldering process starts. R1 is obtained if the assembly through the soldering process is performed with initial flat layers (iteration 1). The DCB interconnected to the baseplate through the lead-free solder material becomes flat, as the soldering process is performed. Nevertheless, the mounting and operation conditions introduce additional bending effects R2 to the system, which can be extracted by simulation (iteration 2). In this case, the consideration of an additional simulation step is necessary (iteration 3), so that the assembly remains flat as good as possible during operation. The principle of the optimization, ie. the different steps needed to minimize risks during operation for a power module baseplate are illustrated in Figure 2.

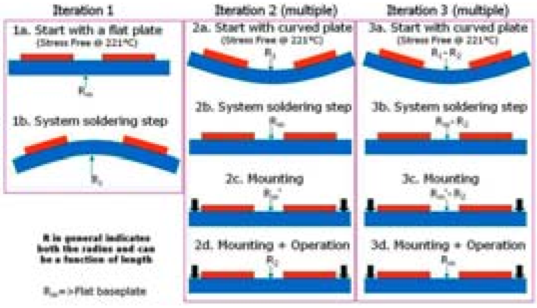

Figure 2: Principle for power module baseplate optimization and steps description

In order to verify the methodology, 6 layouted DCBs soldered to a 3mm thick copper baseplate (162mmX124mm) was considered for simulations. The DCB (56mmX40mm)

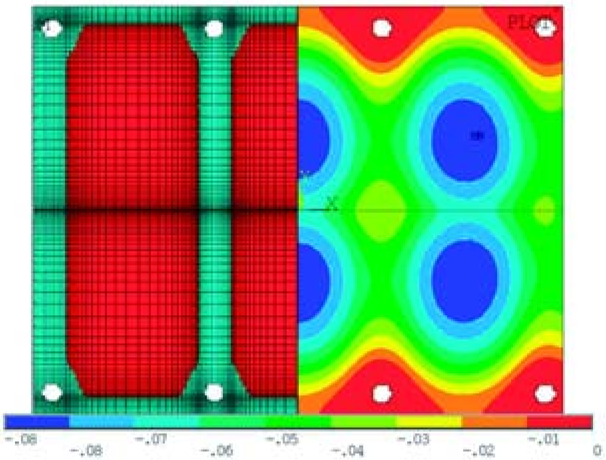

Figure 3: FEM-mesh (half-part) and bow distribution [mm] after optimization process

Experimental vehicle description and bondary conditions consists in a base copper layer of 0.3mm, a ceramic thickness of 0.32mm and a layouted copper layer of 0.3mm. Figure 3 (left side) depicts the mesh of the assembly, the solder layers and the soldered DCBs, performed with the ANSYS FEM package [4]. The solder layers are non-uniform due to the pre-stamped form of the baseplate. Only half of the whole assembly was meshed for calculations due to “quasi-symmetry”. Restrictions in displacements related to symmetry properties were set as boundary conditions. The DCBs were considered without chips and flat for simulation. All material properties were taken linear, except for the copper baseplate, which required extensive elastic-plastic characterization. Material data for the copper baseplate were extracted from UD probe measurements provided by the baseplate material supplier. The characterization was performed with the help of an Instron measurement system.

FEA analysis and simulation results

After the boundary conditions are set, R1 and R2 extracted out of pre-simulation steps, the final iteration for the baseplate optimization is perfomed, like described in figure 2. Figure 3 (left side) show the simulation results of the final bending of the baseplate after mounting operation at 80°C (mean operation temperature), with a fixation moment at each screw of 5kN. The optimized value of the bow during operation conditions is found to be within 80µm along the X-axis as well as along the Y-axis. More specifically, the region areas corresponding to the centre of the DCB (dark up to light blue region) is found “quasi-flat”, allowing the IGBT chips to remain safe during operation. The simulation results could be verified with the help of measurement data out of the experiments. A comparison between simulation and measurement results is provided in figure 4, first at room temperature after soldering process (blue lines), as well as after mounting operations (red lines). In addition, simulation allows the prediction of the bow profile of the baseplate during operation (magenta lines). Else, the simulation results match the experimental data, whereas mainly compressive stress up to 35MPa was found in the DCB under operation conditions.

Conclusion

In this work, an optimized baseplate meeting adequate reliability conditions for individual components was designed using simulations. The simulation results are found in good agreement with data out of experiments. The article also shows the importance of material characterization work, where a high degree of precision of the data used in simulation is necessary to optimize the shape of power module baseplate before assembly processes. In addition, the methodology can provide recommendations regarding the process of thermal paste application. This validates the proposed methodology for baseplate optimization. Further investigations are carried out to understand the impact of parameters like solder thickness, heat sink material, stamping process or pre-bending effects of DCBs on the baseplate bow.

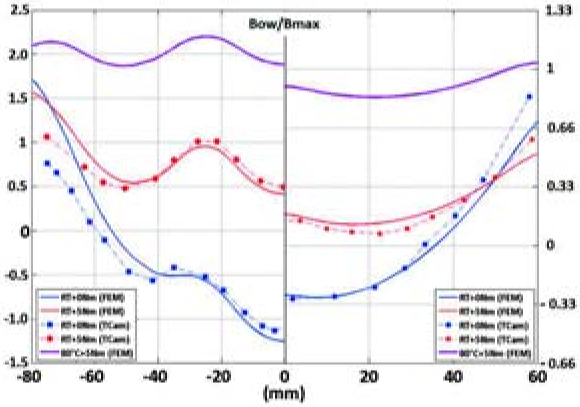

Figure 4: FEA vs. measurement results

Literature

[1] Johann-Peter Sommer, Reinhold Bayerer, Roman Tschirbs, Bernd Michel: „Baseplate Shape Optimisation for High-Power IGBT Modules“, CIPS 2008, pp. 323-326

[2] I. Paul, "Simulationsbasierte Optimierung von Bodenplatten in Leistungsmodulen" 39. Kolloquium Halbleiter-Leistungs-Bauelemente und ihre Systemtechnische Anwendungen 08. - 09. November 2010, Freiburg / Breisgau

[3] P.H.Townsend, D.M.Barnett, and T.A.Brunner. “Elastic relationships in layered composite media with approximation for the case of thin films on a thick substrate” Journal of Applied Physics, 62(11):4438–4444, 1987

[4] ANSYS version 13.0, User’s Manual Reference

www.infineon.com/highpower

New 8-bit Microcontrollers with integrated configurable logic in 6- to 20-pin packages

Microcontrollers

Digital Signal Controllers

Analog

Memory

RF & Wireless

Microchip's new PIC10F/LF32X and PIC12/16F/LF150X 8-bit microcontrollers (MCUs) let you add functionality, reduce size, and cut the cost and power consumption in your designs for low-cost or disposable products, with on-board Configurable Logic Cells (CLCs), Complementary Waveform Generator (CWG) and Numerically Controlled Oscillator (NCO).

The Configurable Logic Cells (CLCs) give you software control of combinational and sequential logic, to let you add functionality, cut your external component count and save code space. Then the Complementary Waveform Generator (CWG) helps you to improve switching efficiencies across multiple peripherals; whilst the Numerically Controlled Oscillator (NCO) provides linear frequency control and higher resolution for applications like tone generators and ballast control.

PIC10F/LF32X and PIC12/16F/LF150X MCUs combine low current consumption, with an on-board 16MHz internal oscillator, ADC, temperature-indicator module, and up to four PWM peripherals. All packed into compact 6- to 20-pin packages.

FAST-START DEVELOPMENT TOOLS

PICDEM™ Lab Development Kit - DM163045

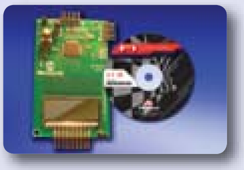

PIC16F193X 'F1' Evaluation Platform - DM164130-1

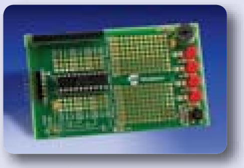

PICkit™ Low Pin Count Demo Board - DM164120-1

Free CLC Configuration Tool:
www.microchip.com/get/euclctool

Go to www.microchip.com/get/eunew8bit to find out more about low pin-count PIC® MCUs with next-generation peripherals

microchip DIRECT
www.microchipdirect.com

www.microchip.com

MICROCHIP

The Microchip name and logo, HI-TECH C, MPLAB, and PIC are registered trademarks of Microchip Technology Inc. in the U.S.A., and other countries. mTouch, PICDEM, PICkit, and REAL ICE, are trademarks of Microchip Technology Inc. in the U.S.A., and other countries. All other trademarks mentioned herein are the property of their respective companies. © 2011, Microchip Technology Incorporated. All Rights Reserved. DS30629A. ME293AEng/09.11

One More Way to increase the Recovery Softness of Fast High-Voltage Diodes

By Chernikov A. A., Gubarev V. N., Stavtsev A. V., Surma A. M., Vetrov I. Y.,
Proton - Electrotex ISC

Due to the development of the power converters based on the high-voltage IGBT and IGCT the demand for the high-voltage fast recovery diodes (FRD). The requirements to the high-voltage FRD of a new generation are as follows to assure:

- stable functioning at high values of di/dt direct current roll-off at reverse recovery (from hundreds to thousands of A/µs), and the current roll-off speed is controlled by inductivity of circuit,
- series characteristic of reverse recovery defined by

$S^* = t_f/t_s$, or by

$$S = \frac{|\,(di/dt)_s\,|_{\max}}{|\,(di/dt)_f\,|_{\max}}, \qquad (1)$$

where t_s and t_f – period of the first and the second phase of reverse recovery, $|(di/dt)_s|_{max}$ and $|(di/dt)_f|_{max}$ – maximum absolute value of **di/dt** at the first and the second phase of reverse recovery.

Despite of SiC power devices fast development, still long time will find a use also silicon diodes, owing to the rather low cost and well fulfilled technology. In particular it concerns to super-power diodes (currents over several hundreds Amps, voltage over several thousand Volt).

The softer characteristic of reverse recovery of silicon FRD, the lower voltage spike at recovery of this device in the circuit with mainly inductive load, and the lower level of electromagnetic noise caused by fast changes (oscillations) of current and voltage during the switching of the module.

To increase the S-factor different special design and technological procedures are being used. The most widespread procedures are local decrease of carrier life time (τ) in the layers of semiconductor element near pn-junction [1-3] and decrease in injection efficiency of pn-junction [3-7]. At that the control of injection efficiency is achieved by increase in recombination whether in emitted layer, or on the surface of the semiconductor element adjacent to the emitter area.

Thus the variation of recombination in various areas of diode element is one of the most effective ways to influence the S-factor.

Physical preconditions and calculations results

To evaluate the influence of the recombination speed change in the layers of the diode element located at different depth, the following method was used. The process of reverse recovery of the high-voltage power diode **p^+-p-n^--n^+** element with "basic" axial distribution τ was simulated with the help of computer. A very thin test layer (r-layer) is fed into the diode element, which has a short life time compared to the "background" layer τ**,** which though had no big influence on concentration distribution of nonequilibrium carriers, which is typical to the "basic" element. If this test layer is fed into at various depth, and thus go through the whole depth of diode, calculated the S-factor change in each case (δ**S**), the effect evaluation of recombination change at different depth can be achieved for that particular characteristic. The above mentioned arguments are surely true to insignificant variations of life time profile.

The results of such calculations for the element of typical power diode are presented at Figure 1. It's clear that **S** increases at local decrease of τ in areas of pn-junction, and as far as the depth of **r**-layer close to the middle of the element, the effect gets negative what complies with the general notion.

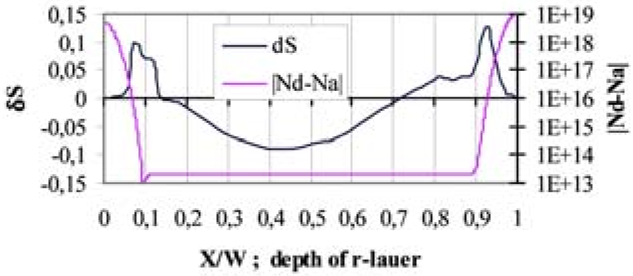

Figure 1: The influence of local recombination change in different depth of diode element on S-factor.

However there is the second area near **n^+** layer where local decrease τ can give the positive effect again. This paradoxical at first sight result can be explained in the following way.

It is well-known that [8] at reverse recovery of **p-i-n** diode in **i-** layer of the semiconductor element two domains with high electric-field strength appear: one is adjacent to the **p**-layer, another to the **n-** layer. This happens at recovery of **p^+-n^- - n^+** diode as well, and the strong electric field in the domain adjacent to the **p^+-n^-** junction is caused by presence of uncompensated electric charge of atoms of donor impurity and holes flowing through **p^+-n^-** junction, and in the domain adjacent to the **n^-- n^+** boarder – by uncompensated charge of excess electrons appearing with flow of electron current through the domain. And to build the domain adjacent to the **n^-- n^+** boarder rapid decrease in concentration of electron-hole pairs required in this area, i.e. local decrease τ near the **n^-- n^+** boarder contributes to the building of domain with high electric-field strength.

Influence of domain adjacent to the **n^-- n^+** boarder on the character of reverse recovery was well studied [3, 9]. It's proven that during the process of reverse recovery the width of both domains increases which leads to domains linkage in the **n^-** layer. As a result, "snappy recovery" occurs, i.e. the negative influence of domain building on **S-**factor, adjacent to the **n^-- n^+** boarder.

However our calculations show that in case if domain linkage doesn't happen, the peak reverse recovery current (**I_{rrM}**) and maximum rate of rise of on-state current (**max |(di/dt)$_f$|**) can be decreased as a result of reassignment of applied to the diode voltage between domains.

The calculations were made with the help of "ISTOK" software used for computer modeling of semiconductor devices characteristics:

- The thickness of the silicon wafer – 640 µm, element surface – 14 cm²,
- Electron concentration in n- layer - 1.5*10^{13} cm^{-3}, concentration profile of dopant impurity in p and n+ layers is shown in Figure 2à.
- Carriers' life time close to **n$^-$- n$^+$** border was locally decreased in comparison with its value in other parts of n- layer (Figure 2à., curve "carrier life time (1)").

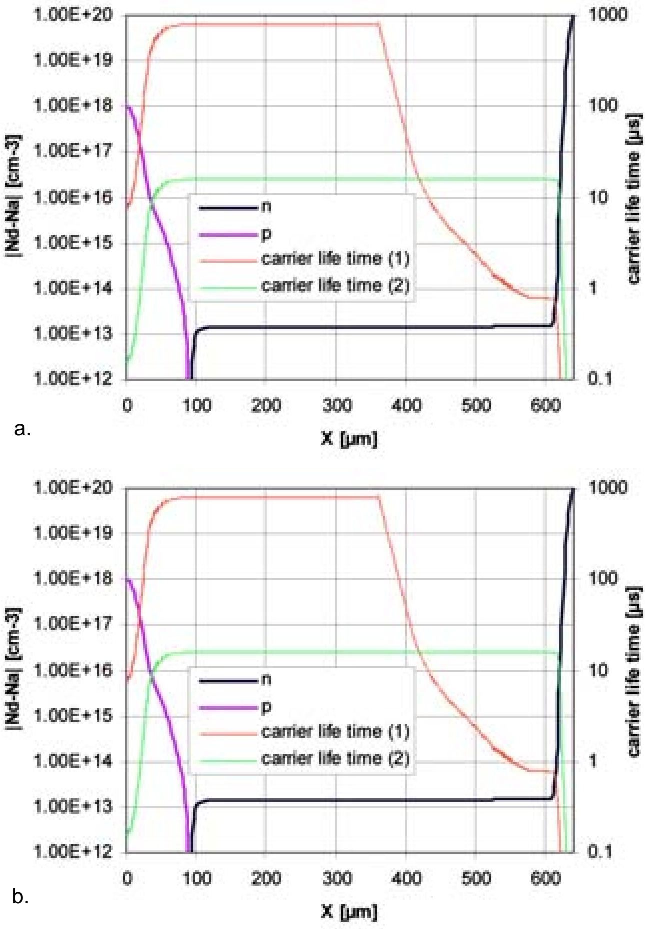

*Figure 2: Concentration profile of dopant impurity for diode element used in calculations: a. – without **n'** layer; b. - with **n'** layer.*

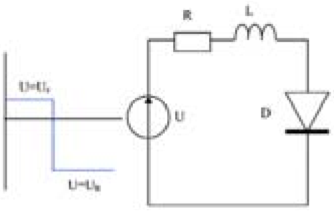

Figure 3. The test circuit used in calculations.

The diode element was added to the loop shown in Figure 3, **R**=0.05 Ω, **L**=0.6 µH, **V_F**=50 V, **V_R**=-1000 V. Direct current was about 1000 A, and **(di/dt)$_s$** about -1670A/µs.

Characteristic curve of current and voltage at reverse recovery is shown in Figure 4, S= 5.2. In Figure 5 and Figure 6 intensity of electric field and excess-carrier density distribution through the thickness of the semiconductor element in different time periods are shown.

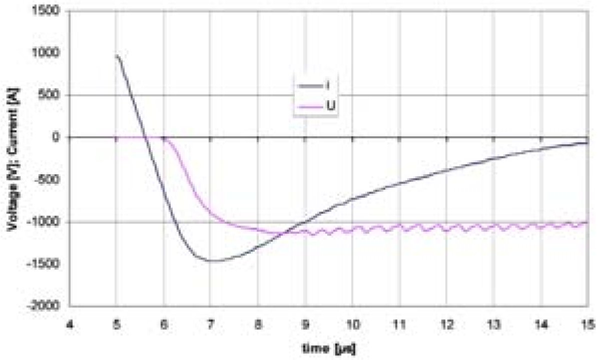

Figure 4: Characteristic curve of current (i) and voltage (U) at reverse recovery. Concentration profile of dopant impurity – Figure 2a; profile of τ - Figure 2a, curve "carrier life time (1)"

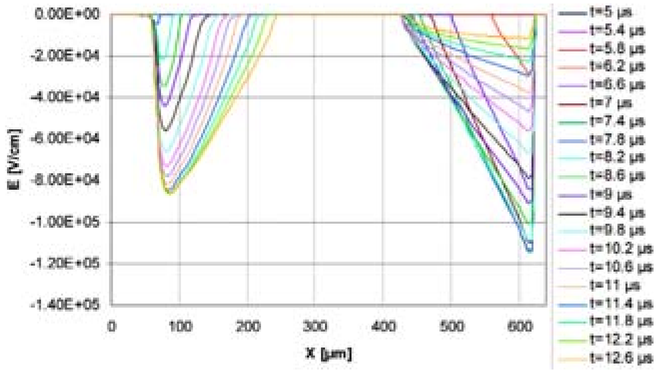

Figure 5: Distribution of electric field in diode element at different time periods. Concentration profile of dopant impurity – Figure 2a; profile of τ - Figure 2a, curve "carrier life time (1)"

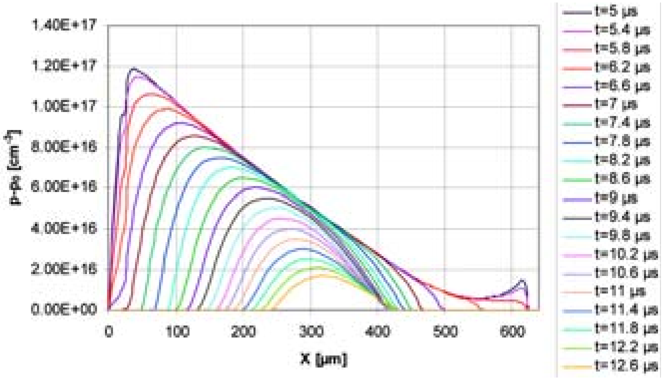

Figure 6: Excess-carrier density distribution in diode element at different time periods. Concentration profile of dopant impurity – Figure 2a; profile of τ - Figure 2a, curve "carrier life time (1)"

According to Figure 5 it's clear that the strong electric field area near the **n$^-$- n$^+$** border initiates earlier than the same area near **p-n** junction. And exactly the strong electric field limits the peak reverse recovery current and the rate of current change in the beginning of the second phase of reverse recovery. Further smoothly decreases reverse voltage in the area of strong electric field near **n$^-$- n$^+$** border (**U_n**), and smoothly increases reverse voltage in the area of strong electric field near **p-n** junction (**U_p**), as shown in Figure 7.

Importance of the above described processes to ensure soft recovery are illustrated by the results of the comparative analysis of diode reverse recovery with similar semiconductor element, but with even distribution of τ in $\mathbf{n}^-$ layer.

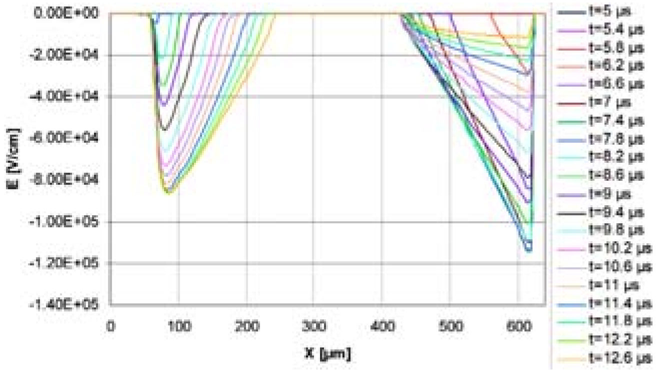

*Figure 7: Time dependences of partial voltages in diode element at reverse recovery: $\mathbf{U_n}$ - the voltage of strong electric field area near the $\mathbf{n}^-$- $\mathbf{n}^+$ border, $\mathbf{U_p}$ - the voltage of strong electric field area near **p-n** junction. Concentration profile of dopant impurity – Figure 2a; profile of τ - Figure 2a, curve "carrier life time (1)"*

The value of τ was higher than minimal and lower than maximum τ in case with uneven distribution, and was selected to ensure he closest value of peak reverse recovery current.

In Figure 8 – Figure 10 characteristic curves of current and voltage are shown, as well as the distribution of electric field intensity and excess-carrier density according to the thickness of silicon element. Same curves for $\mathbf{U_n}$ and $\mathbf{U_p}$ are shown in Figure 11.

According to the above shown figures the area of strong electric field near **n-- n+** border appears in this case as well, however reverse voltage in this area is relatively low. Diode reverse recovery has lower softness in this case (**S**=0,76).

It's well-known that during the proton ray treatment recombination centers appear in silicon which decreases τ, and also doping centers of donor type induced by H-atoms and similar atoms of "traditional" dopants [9]. Herewith axial concentration distribution of recombination centers as well as H-induced donors has maximum near the end of proton path.

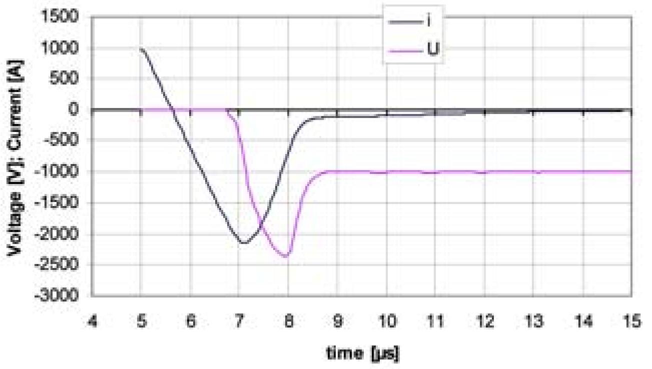

Figure 8: Characteristic curve of current (i) and voltage (U) at reverse recovery. Concentration profile of dopant impurity – Figure 2a; profile of τ - Figure 2a, curve "carrier life time (2)"

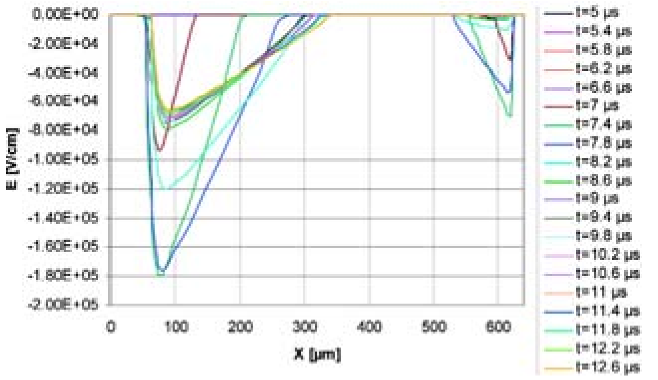

Figure 9: Distribution of electric field in diode element at different time periods. Concentration profile of dopant impurity – Figure 2a; profile of τ - Figure 2a, curve "carrier life time (2)"

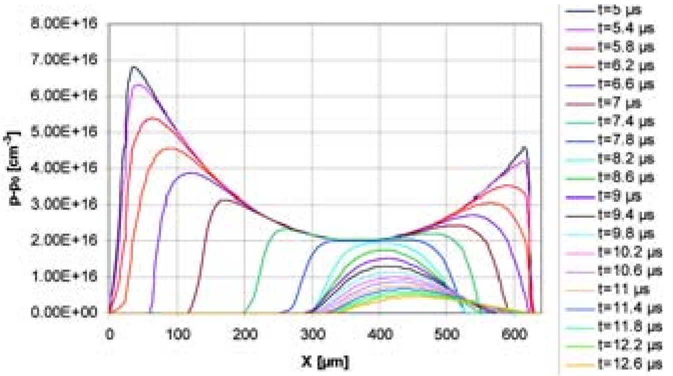

Figure 10: Excess-carrier density distribution in diode element at different time periods. Concentration profile of dopant impurity – Figure 2a; profile of τ - Figure 2a, curve "carrier life time (2)"

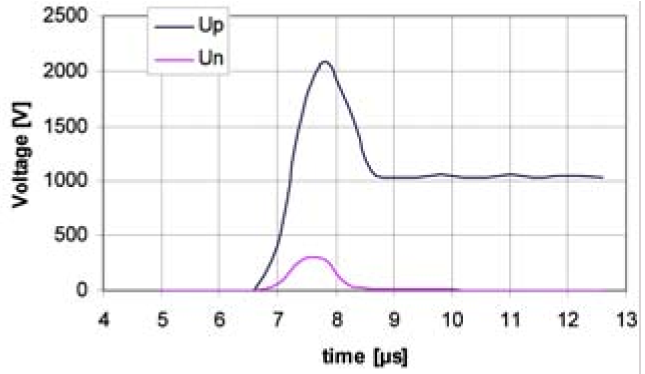

Figure 11. Time dependences of partial voltages in diode element at reverse recovery: Un - the voltage of strong electric field area near the n— n+ border, Up - the voltage of strong electric field area near p-n junction. Concentration profile of dopant impurity – Figure 2a; profile of τ - Figure 2a, curve "carrier life time (2)"

In [2, 11] it's shown that using high-power proton irradiation through the additional screen, which is used to control the depth of proton path in the silicon element, a wide area with implanted H-atoms can be achieved. This area has a low specific resistance as a result of H-induced donors presence. Moreover, this method allows dimensionally separate the maximums of recombination centers and H-induced donors. Thus, at Figure 12 the axial value distribution is shown, which characterizes the effective concentration of recombination defects and the concentration distribution of the implanted hydrogen at proton ray treatment of the silicon element with initial energy of 24 MeV. The concentration of the additional donors at maximum distribu-


60
5
10
15
20
25
30
35
40
45
50
55
30
5
15
20
25

tion can be controlled with high accuracy (error less than 1%) even at absolute values equal to the concentration of phosphorus in the n-layer (N*10^{13} cm^{-3}).

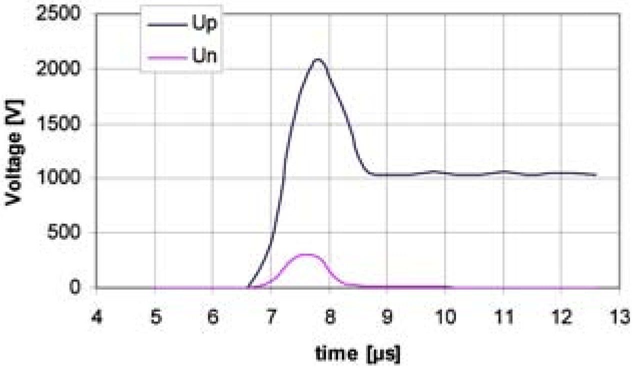

*Figure12. The axial distribution of values **$(1/\tau-1\tau_0)/(1/\tau-1/\tau_0)_{max}$** and the concentration distribution of the implanted hydrogen at proton ray treatment of the silicon element with initial energy of 24 MeV.*
*1- **$(1/\tau-1\tau_0)/(1/\tau-1/\tau_0)_{max}$**; 2 - **$N_{hydrogen}/(N_{hydrogen})_{max}$·$R_p$** – the path length of proton in silicon, τ_0 and τ - carrier life time values before and after proton irradiation, the index "max" corresponds to values in a point of maximum.*

Thus, such way of the proton irradiation of the silicon element from the side of the **n^+** layer and "hidden" super-soft **n'**-buffer can be built within **n^-** layer.

The calculations show that the influence of such hidden layer on **S**-factor is quite ambiguous and depending on the characteristics of the semiconductor element and recovery process condition, presence of this layer can lead to decrease or to increase of **S** as well.

In Figure 13 and Figure. 14 characteristic curves of current and voltage are shown, as well as the electric field distribution through the thickness of the semiconductor element of diode similar to Figure 2, but containing buffer **n'** layer. Concentration distribution of dopants in this layer was close to shown in Figure 12, and the maximum concentration equaled 1*10^{14} cm^{-3} at depth of 50 µm from anode surface. Corresponding curves of U_n and U_p are shown in Figure 15.

It's clear that presence of **n'** layer leads to increase of area width of strong electric field near **n^-- n^+** boarder. On the one hand, this increases danger of area linkage of strong electric field and snappy recovery. To avoid it the thickness of the element with **n'** layer should be higher than the thickness of the similar element without such layer.

The necessary condition for area of strong electric field in n^- or **n'** layer to appear is breaking of electrical neutrality with current flow density above some critical rates

$$j_n > j_{crit} = q \cdot n_0 \cdot v_{ns} \quad , \qquad (2)$$

q – electron charge, **n_0** - equilibrium density of electrons, **v_{ns}** – max electron speed in strong electric field. As a result within **n'** layer area of strong electric field appears with relatively higher current density than for n- layer. This leads to increase of maximum surge current value at reverse recovery (**I_{rrM}**) of element with **n'** layer in comparison with similar element without this layer. Same thing happens when current drops in second phase of reverse recovery electric field intensity within **n'** layer decreases rapidly (Figure 14) what leads to rapid decrease of **U_n** (Figure 15).

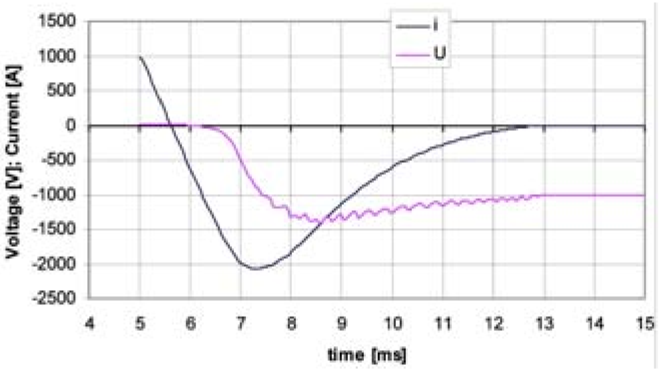

Figure 13. Characteristic curve of current (i) and voltage (U) at reverse recovery. Concentration profile of dopant impurity and profile of τ - Figure 2b

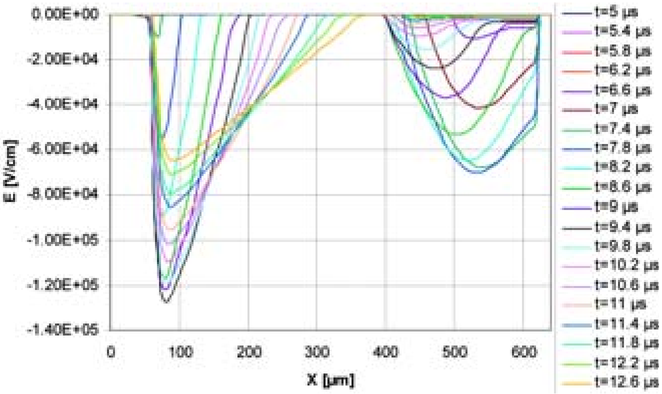

Figure 14: Distribution of electric field in diode element at different time periods. Concentration profile of dopant impurity and profile of τ - Figure 2b

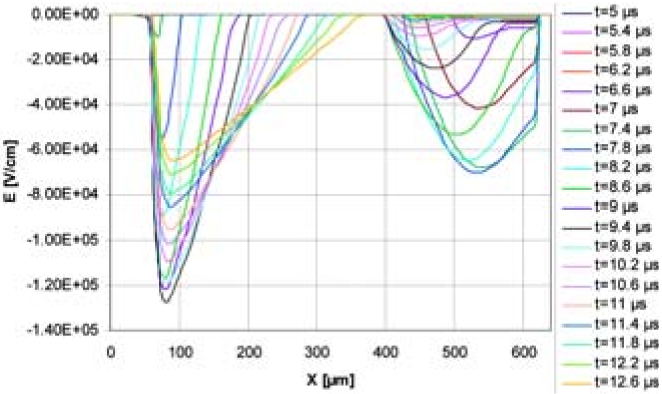

*Figure 15: Time dependences of partial voltages in diode element at reverse recovery: **U_n** - the voltage of strong electric field area near the **n^-- n^+** border, **U_p** - the voltage of strong electric field area near **p-n** junction. Concentration profile of dopant impurity and profile of τ - Figure 2b.*

The following factors differently influence on **S**-factor: increased thickness of strong electric field area helps increase of **U_n** and **S**, rise delay and further rapid drop of electric field intensity within **n'** layer – decreases **S**. For a certain example inletting into the element of **n'** layer leads to decrease of **S** to 2.2. However with increase of **$|(di/dt)_s|$** and consequently of **I_{rrM}**, and **V_R** as well (Figure 3), the situation can change.

In Figure 16 changes of **S**-factor are shown in dependence of $\mathbf{V_R}$, with reverse recovery on induction load, $\mathbf{|(di/dt)_s|}$ = 5000 A/µs for elements with n' layer and without it. Also the changes of $\mathbf{(U_n)_{max}/V_R}$ for both cases are shown there. $\mathbf{(U_n)_{max}}$ corresponds to absolute maximum Un during the whole reverse recovery process.

It's clear that **S** is high till $\mathbf{(U_n)_{max}/V_R}$ is about 1. Increasing $\mathbf{V_R}$, to some point this value is getting low, and as a result **S** is decreasing as well. It ought to be noted that $\mathbf{V_R}$ when $\mathbf{(U_n)_{max}/V_R}$ starts to decrease is higher for element with **n'** layer than for similar element without it. Thus, **S** is higher when $\mathbf{V_R}$ has increased value (on condition that there is no linkage of strong electric field areas).

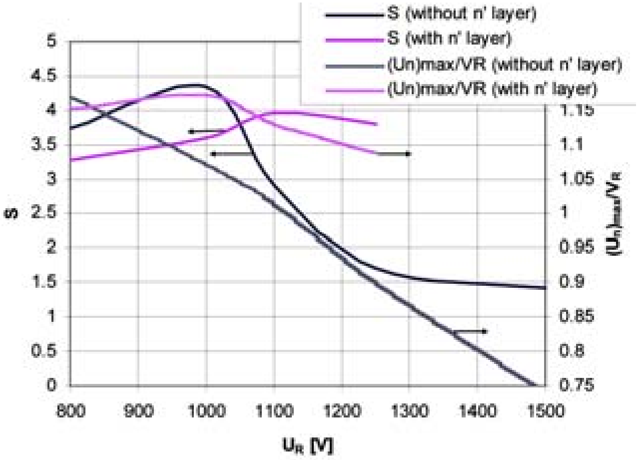

Figure 16: Changes of S-factor and $\mathbf{(U_n)_{max}/V_R}$ *in dependence of* $\mathbf{V_R}$ *for elements with* ***n'*** *layer and without it. Reverse recovery on induction load,* $\mathbf{|(di/dt)_s|}$ *= 5000 A/µs.*

Experimental results

Experimental diodes were produced on the base of the original neutron transmutated silicon with specific resistance of 350 Ω*cm and depth of 640 µm. The **p** – layer was formed by co-diffusion of **B** and **Al** at a depth of ~30 and 90 µm accordingly, and the $\mathbf{n^+}$ layer by the diffusion of phosphorus at a depth of 20 µm. The diameter of the silicon element of the ready-made diodes equaled 56 mm.

The diode elements were proton irradiated according to the above mentioned method for formation in the n- layer, not far from the cathode of the hidden super-soft layer, and also the layer with decreased τ adjacent to the boarder of the $\mathbf{n^+}$ layer. After the ray treatment the elements were annealed to activate the H-induced donors and aligning of τ. The $\mathbf{U_{Rbr}}$ of the diodes after all treatment was 4600-4800 V.

Typical oscillograms of reverse recovery current of the experimental diodes are displayed at Figure 17. At Figure 17a. the process of recovery in the edge of low reverse voltage (100V) and current roll-off speed about 150 A/µs is shown. The value of **S**-factor in this case is about 1. It should be mentioned as a characteristic feature the increased period with smooth change of current near maximum.

At Figure 17b. the process of reverse recovery at V_R = 1000 V is shown. The initial direct current is about 1000 A, roll-off speed is about 1600 A/µs. Typical values of **S**-factor were 2, no snappy-effect registered.

It has to be mentioned that current and voltage characteristic curves, which were experimentally achieved, are very close to calculation data (Figure 13).

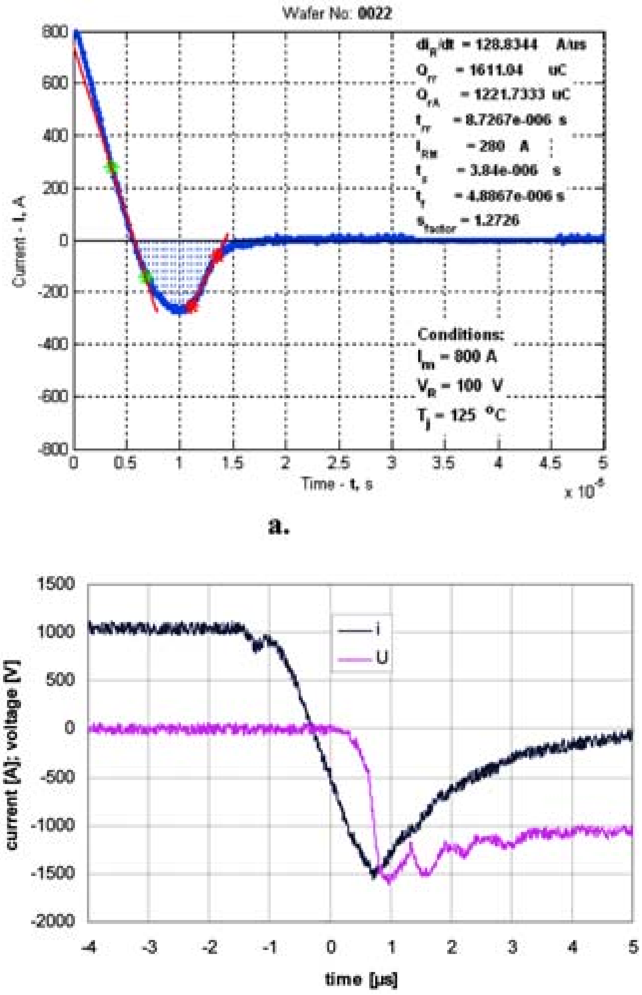

Figure 17: Typical oscillograms of experimental diode reverse recovery: a. – $\mathbf{V_R}$ = 100 V, $\mathbf{|(di/dt)_s|}$ = 150 A/µs: b. - $\mathbf{V_R}$ = 1000 V, $\mathbf{|(di/dt)_s|}$ = 1600 A/µs.

Conclusion

The possibility in principle to develop fast p-n-n$^+$ diode with soft recovery by local decrease of τ near the border of $\mathbf{n^+}$ layer was displayed.

Soft reverse recovery with high rates of anode current roll-off and reverse voltage can be assured with the help of forming the hidden buffer **n'** layer in semiconductor element. The layer with decreased τ and hidden buffer **n'** layer can be formed simultaneously by proton irradiation.

References

[1] J. Lutz, U. Scheuermann, Advantages of the new controlled axial life-time diode. Proc. PCIM'94, Nurnberg, 1994.

[2] V. A. Potaptchouk et al. Distinctions of Lifetime Damage in Silicon Diode Layers at Various Radiation Processing: Influence on Power Losses and Softness of Reverse Recovery Characteristic. PCIM'2002, Nurnberg, 2002, pp. 293-299.

[3] M. T. Rahimo, N. Y. A. Shammas. Optimisation of the reverse recovery behaviour of fast power diodes using injection efficiency techniques and lifetime control techniques. EPE'97, Trondheim, 1997, pp 2.99-2.104.

[4] M.T. Rahimo, N.Y.A. Shammas, Emitter design effects on soft/snappy recovery in modern fast power diodes. ISPS'96, Prague, 1996, pp. 65–71.

[5] Rahimo M.T., Crees D. E., Shammas N.Y.A A novel concept for fast recovery diodes having junction charge extraction (JCE) regions. ISPS, 1998.

[5] Kitagawa M., Matsushita K. , Nakagawa A. High Voltage 4 kV Emitter Short Type Diode (ESD). ISPSD, 1992 pp. 60-65.

[6] H. Schlangenotto, J. Serafin, F. Sawitzki, H. Maeder. Improved recovery of fast power diodes with self-adjusting P-emitter efficiency. IEEE Electron Devices Letters, 1989, July, pp. 322-324.

[7] Benda, Spenke. Reverse recovery processes in silicon power rectifiers, IEEE Trans. on Electron Devices ,1967, pp. 1331–1354.

[8] V.V. Kozlovski. Modification of semiconductors by proton beam. S.-Pb., Nauka, 1993.

[9] M. T. Rahimo, N. Y. A. Shammas. Freewheeling Diode Reverse-Recovery Failure Modes in IGBT Applications. IEEE Trans. on Ind. Appl., 2001, v. 37, No. 2, pp. 661-670.

[10] A. Y. Semenov et al. Series of Fast Thyristors with Controllable Reverse Recovery Charge and Technological Complex of Proton Irradiation for Control of Their Switching Characteristics. PCIM'2003, Nurnberg, 2003, pp. 509-514.

www.proton-electrotex.com

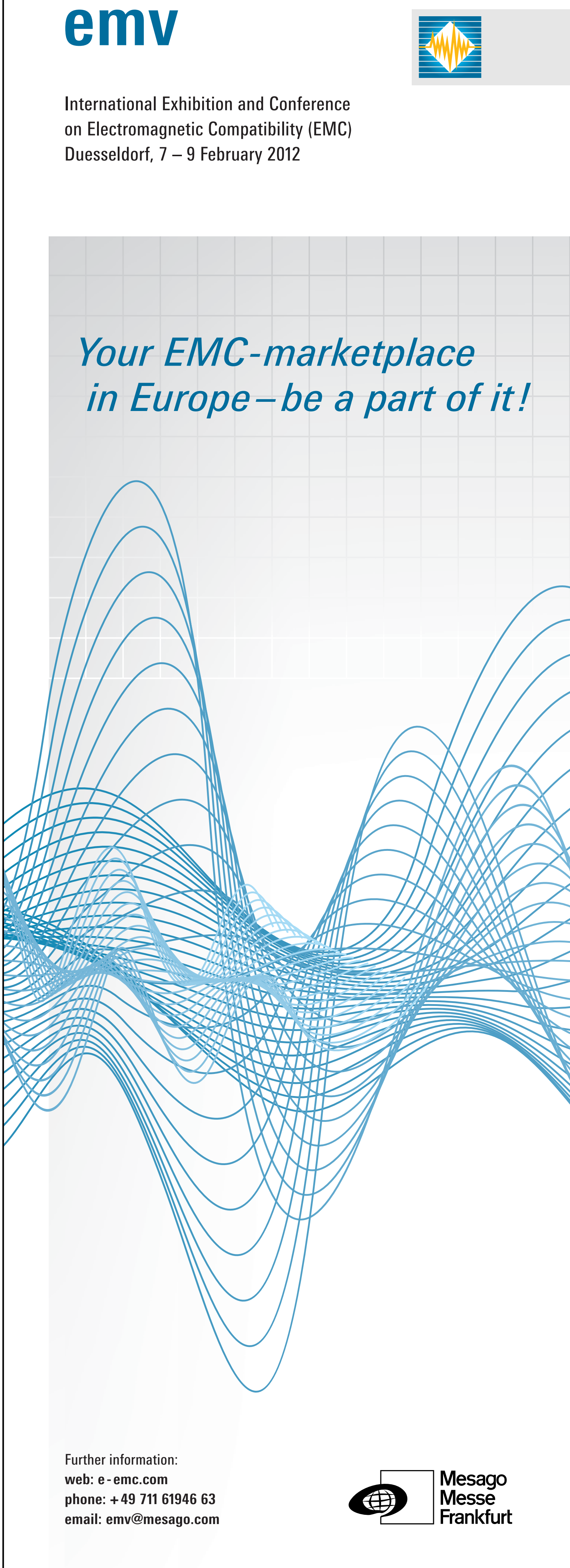

IGBTs in Reverse Gear

The complex interplay of freewheeling diodes and IGBTs

State-of-the-art power semiconductors are intended to switch quickly in order to reduce dynamic losses. Once an IGBT turns off, the load current commutates to the freewheeling diode. To avoid undesirable side-effects , these two semiconductors have be very well matched in terms of their electrical properties.

By Stefan Schuler, Development Engineer and André Müller, BA student, SEMIKRON

Electronic circuits are usually designed such that no IGBT has to be operated in reverse direction. The problem is, however, that situations occur in applications in which this is exactly the case, at least for a transitional period. Figure 1 shows two half bridges connected via a load inductance L_L. The switches T_3 and T_2 are conducting; a current i_L flows through the load inductance. Let us now take a closer look at the point in time at which T_2 turns off: current i_L begins to commute from T_2 to the freewheeling diode D_1. This produces a voltage overshoot induced by the diode turn-on behaviour. Depending on the current rate of rise di/dt, this voltage may briefly amount to as much as several hundred Volt; this is also referred to as the diode „forward recovery time“. At the same time, the emitter potential of T_1 is higher than that of the collector – the IGBT is now in actual fact poled in reverse direction.

The question which arises in this context is whether the voltage amplitude and forward recovery duration may be dangerous for the antiparallel IGBT.

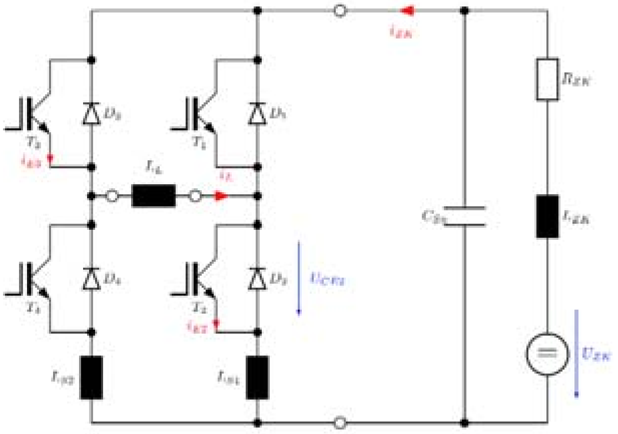

Figure 1:Two half bridges connected via a load industance L_L

Forward recovery time

A basic high-voltage diode comprises a p^+-n^--n^+ layered structure, where the middle zone is far bigger and often weakly doped only. In Punch-Through (PT) diodes, the width of the middle zone, as well as the doping of this region, is selected such that he field strength is only partially reduced until the n^+ region is reached – here it drops continously down to zero, but it must never go beyond the edge. In order to switch these diodes from blocking to conducting state, the electron-hole plasma first has to be formed in the middle zone. To do so, electrons and holes are injected from the adjacent n^+- and p^+zones. This process is, however, somewhat sluggish, meaning a high forward recovery voltage U_{fr} is produced perpendicular to the middle zone when a sudden current is applied to the diode. This is typical of inductive loads. The amplitude of this voltage depends on the voltage class of the diode, as well as the diode technology. For higher voltage classes the middle zone is larger and thus slows down the process of plasma formation significantly. Figure 2 shows the voltage curve for various di/dt of a 1200V diode. As the current rate of rise increases, the time and amplitude of the maximum move towards earlier and higher values. A rate of rise measured in a harsh lab test and barely achievable in practice amounting to 32kA/µs even causes the forward voltage to exceed the 200V mark briefly. It goes without saying that this high value is a theoretical value more than anything else and in practice the maximum values are in the region of 8…10kA/µs.

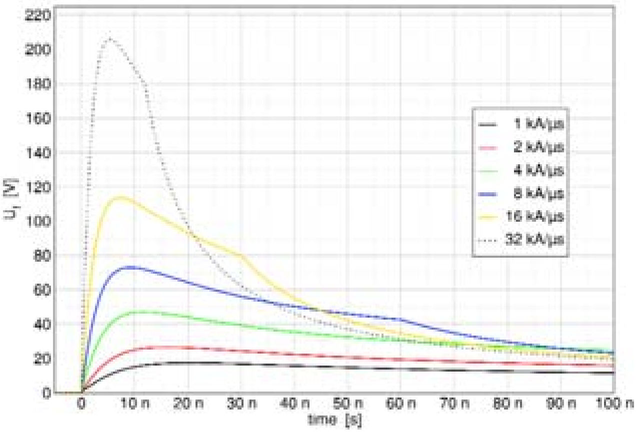

Figure 2: Recovery times of a 75A/1200V power diode for various di/dt and I_{max} of 480A.

Shift into reverse gear

For negative collector-emitter voltage, the pn junction between the p^+substrate and the n buffer blocks, thus preventing current flow. Normally, however, IGBTs are not optimised for reverse operation [1], which is why the blocking capability of this pn junction is poor and breakdown occurs at some 10V already. In this case, the IGBT is filled with electron-hole plasma due to the emitter-side pn junction and goes into an uncontrolled state [2]. As with the diode, this takes a finite time and depends on how long the charge carriers need to distribute themselves in the weakly doped n^-zone.

A further factor to be born in mind in relation to IGBTs is the critical field distribution at the p-wells owing to their finite curvature [3], especially at the edge of the chip. Here, an excessive local field strength increase occurs during operation which may result in what is known as lateral breakdown rather than vertical breakdown triggered by the avalanche effect of one or more IGBT cells. A possible countermeasure are field plates. However, usually several p-doped guard rings for junction termination (at the edge zone) are implemented. This enables high blocking voltages to be achieved in forward direction without the risk of lateral breakdown.

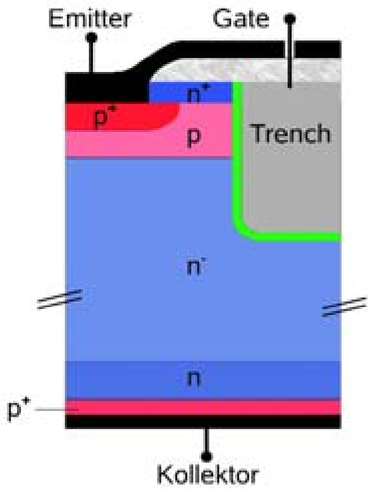

Figure 3: Schematic of a Trench IGBT in Field Stop technology.

Nevertheless, in reverse operation the conditions are different, since for the junction termination to be effective the underside of the wafer would have to be doped; for technical reasons, however, this is not done.

In conclusion, it can be said that there are two essential weakpoints for reverse operation: on the one hand, the lack of an junction termination for reverse operation and the plasma-induced instability, on the other hand.

Dielectric strength

Accordingly, the external IGBT conditions are dictated by the switching properties of the antiparallel diode. For a diode with ideal behaviour, there would be no forward recovery time and thus no overvoltage on turn-on. Owing to the light doping in the middle zone and the need for electron-hole plasma formation first, real power diodes have real delay times which lead to voltage drops as a result of the externally impressed di/dt. By common definition [4], according to which

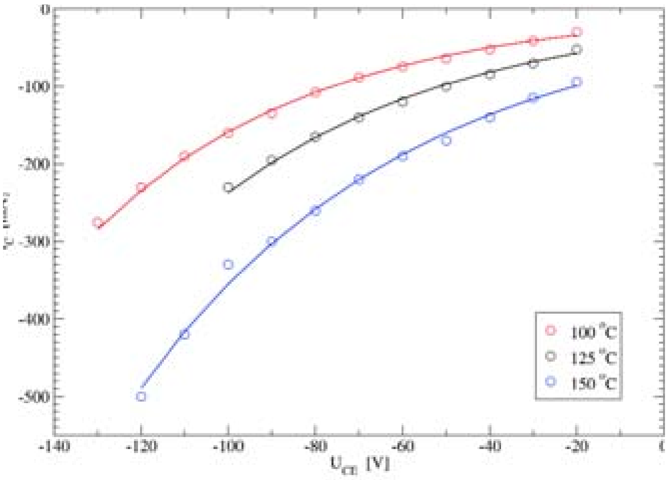

Figure 4: IGBT reverse current vs. the applied voltage for various temperatures (pulse duration per 20ms reading).

time is calculated from the point at which the voltage reaches 10% of the flow voltage U_f up to the point where the voltage has dropped once again to a factor of 1.1 of the U_f, the forward recovery time t_{fr} may amount to as much as several 100 ns, depending on the diode being used.

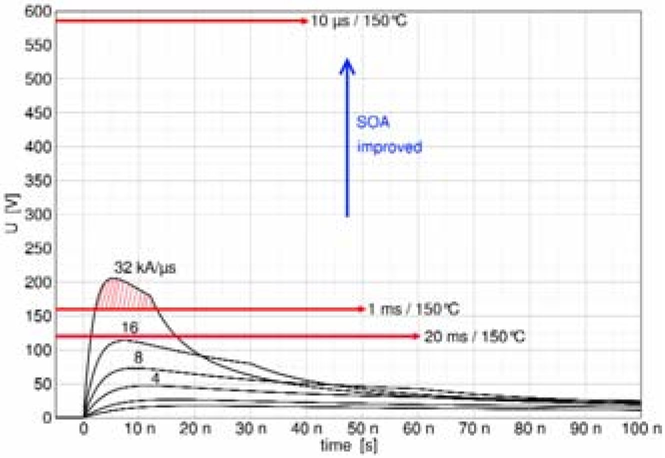

Figure 5:Safe Operating Area (SOA) of the antiparallel IGBT4 at 150 °C for pulse widths of 20ms, 1ms and 10µs, in relation to the forward recovery time of a CAL4 power diode (75A/1200V).

Put to the test

In the tests conducted, voltage pulses of various amplitudes and duration are applied to an IGBT poled in reverse direction. The chip temperature was also varied using a heatable base plate. The chosen pulse duration is 20ms, 1ms and 10µs. The first two durations may seem disproportionately long as regards the actual time needed for forward recovery. They are taken, however, in order to illustrate how much time is needed for plasma formation in the n zone of the IGBT. After all, the better reverse voltage capability for short pulses can be explained by the fact that an approximately equal number of charge carriers then have to be moved in a shorter period of time.

The voltage amplitude is then gradually increased until the protective circuit is triggered. The protective circuit is required to stop the IGBTs from being destroyed and thus enable the IGBT behaviour under different parameters to be tested. The current increases exponentially with the voltage amplitude (Figure 4). At higher temperatures additional displacement occurs, resulting in higher currents. At a chip temperature of 150°C and an applied voltage of 120V, for example, the current measured amounts to as much as 500mA.

In a subsequent test on numerous IGBTs, voltage pulses of gradually increasing amplitude are applied until the IGBTs are distroyed. The results of this test are given in Figure 5 in the form of horizontal lines showing the maximum possible voltage amplitude for a specific pulse duration. This figure also shows the voltage curves resulting from the forward revovery times for the diode under observation. If a horizontal line lies above the diode voltage curve for a defined di/dt, the situation can be deemed sufficiently safe for the IGBT. A remarkable fact here is that, owing to the slow rate of plasma formation, the safety margin increases as the pulse duration decreases.

For pulse durations of 1ms and 20ms commutation above 16kA/µs is still in the critical region. For a pulse duration of 10µs, however, this is clearly no longer the case. Taking the more realistic case of 10kA/µs, the safety margin increases six-fold for a defined pulse duration of 10µs.

Conclusion

In state-of-the-art low-inductance power modules, high commutation rates of rise (di/dt) to the freewheeling diode are already applicable. Here, it is imperative that the resulting forward recovery voltage does not cause breakdown of the antiparallel IGBT, since this would inevitably lead to the destruction of the module.

The extreme current rates of rise tested here are intended to demonstrate the inherent difficulty in forward recovery and the resulting load placed on the antiparallel IGBT. Having said that, the high di/dt used in the lab tests are virtually impossible to achieve in field conditions. Similarly, the constant amplitude and pulse duration used for the IGBT here are both more extreme than in actual field applications. These facts should not be forgotten when evaluating the 6-fold safety margin.

Given the development of new and fast electronic switches and layouts with short switching paths and low paristic inductances, this problem will have to be tackled sooner rather than later. Indeed, well matched IGBTs and diodes are an absolute must if the „reverse gear“ is not to fail us in the future.

Literature

[1] Dr.-Ing. Günter Schmitt: Ansteuerung von Hochvolt-IGBTs über optimierte Gatestromprofile; Dissertation 2009
[2] Prof.Dr.-Ing. N.Kaminski: Leistungselektronik und Stromrichtertechnik I; Vorlesungsskript Universität Bremen 2009
[3] Dr. Ulla Knipper: Untersuchungen zur Robustheit von IGBT-Chips im Lawinendurchbruch; Dissertation 2011
[4] Josef Lutz: Halbleiter-Leistungsbauelemente, Springer-Verlag 2006

www.semikron.com

CONCEPT
INTELLIGENT POWER ELECTRONICS

New 3.3kV SCALE-2 IGBT Driver Core

2SC0535T2A0-33

The new dual-channel IGBT driver core 2SC0535T for high voltage IGBT modules eases the design of high power inverters. Using this highly integrated device provides significant reliability advantages, shortens the design cycle and reduces the engineering risk. Beside the cost advantage resulting from the SCALE-2 ASIC integration, the user can consider to have a pure electrical interface, thus saving the expensive fiber optic interfaces. The driver is equipped with a transformer technology to operate from -55°..+85°C with its full performance and no derating. All important traction and industrial norms are satisfied.

SAMPLES AVAILABLE!

CT-Concept Technologie AG, Renferstrasse 15, CH-2504 Biel, Switzerland, Phone +41-32-344 47 47

Features

Highly integrated dual channel IGBT driver
2-level and multilevel topologies
IGBT blocking voltages up to 3300V
Operating temperature -55..+85°C
<100ns delay time
±4ns jitter
±35A gate current
Isolated DC/DC converter
2 x 5W output power
Regulated gate-emitter voltage
Supply under-voltage lockout
Short-circuit protection
Embedded paralleling capability
Meets EN50124 and IEC60077
UL compliant

www.IGBT-Driver.com

Energy Harvesting Systems Power the Powerless

Energy harvesting solutions allow electronics to operate where there is no conventional power source and without the need to run wires or make frequent visits to replace batteries. This article provides an overview of energy harvesting applications and their benefits, how they work, and the challenges that designers must address to implement them.

By Bakul Damle, Business Director, and Moe Rubenzahl,
Executive Director of Internet Marketing, Maxim Integrated Products

Modern electronic systems solve so many difficult problems that they often seem like magic. Nonetheless, these systems all have the same basic limitation: they need a source of electrical power! Most of the time this is a straightforward challenge for the electronic designer, because there are many power-delivery solutions. Yet sometimes a device has no direct power source, and running wires or replacing batteries is impractical. Even when long-life batteries are usable, they eventually need to be replaced, which requires a service call.
Enter energy harvesting. Energy harvesting (also known as power harvesting or energy scavenging) allows electronics to operate where there is no conventional power source. It eliminates the need for wires or replacement batteries.

This article discusses energy harvesting and its applications. It explains how the process works and the challenges that designers must address to implement a fully functional solution.

What Is Energy Harvesting?

Energy harvesting uses unconventional energy sources to power circuitry. Typically, a tiny energy source is converted to electricity and stored in a durable storage cell such as a capacitor, super capacitor, or microenergy cell (MEC) which is a form of lithium solid-state battery. The system generally includes circuitry to manage the power and protect the storage device and other circuitry.

Sources of energy (Figure 1) include light, captured by photovoltaic cells; vibration or pressure, captured by a piezoelectric element; temperature differentials, captured by a thermoelectric generator; radio energy (RF); and even biochemically produced energy, such as cells that extract energy from blood sugar.

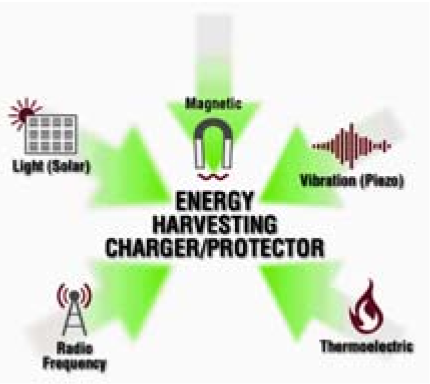

Figure 1: Energy harvesting uses unconventional sources to power circuitry

Energy Harvesting for Remote and Portable Applications

While energy harvesting can be considered “free energy,” energy cost is not what motivates most solutions. Modern energy harvesting is used because it eliminates the need to run expensive power cables to remote locations or the need to replace expensive primary batteries frequently. In simple terms, energy harvesting systems are more convenient and reduce costs for many applications.

There is, however, more to their appeal. Energy harvesting systems are also ResourceSmart® designs. They eliminate wasteful batteries and long powerline runs. They keep systems running without inconvenient, disruptive service calls. They enable monitoring and control at remote locations and especially in sensitive ecological settings.

Applications for energy harvesting focus on management of remote sites, systems, and mobile devices. Typical uses are control of remote sensors, remote wireless sensing devices, asset tracking and personnel identification systems for building access, and enhanced security at remote locations. Specific examples include energy supplied for remote valves for pipelines, irrigation, and other systems that include plumbing but no power; safety and control equipment that monitors oil and gas pipelines; electrically operated automatic flush toilets; wearable electronics attached to clothing or protective gear; surgically implanted electronics such as drug-delivery, monitors, and pacemakers; and smart cards, which contain circuitry but no power source. Energy harvesting is also proving useful with a variety of real-time clock (RTC)/memory backup applications and asset tracking or identification.

The Technical Challenges of Energy Harvesting

Energy harvesting solutions demand much from the electronics that support them. Consider some of these design challenges. If the energy resource is not always present, then the system needs to store energy in a battery, super capacitor, or microenergy cell. Moreover, since energy sources vary, the system must convert, regulate, and control that energy. The circuitry and the energy storage cell must all be protected from excess voltage or power spikes. The supporting electronics must be highly power efficient since the energy source is generally small.

It is also quite clear that remote systems powered by energy harvesting must be very reliable. A service call quickly negates any advantage of the remote control. Finally, remote systems often lack climate control or are subject to fluctuating environmental/temperature conditions. Any energy harvesting system must accommodate and operate flawlessly under those conditions.

Energy Harvesting for the Future

The Maxim® MAX17710 energy-harvesting charger and protector is a new-generation power-management IC that “harvests” the energy generated from a variety of poorly regulated energy-harvesting sources (Figure 1). The MAX17710 provides the energy harvesting and power management to maximize, protect, and control the energy stored in microenergy cells, such as Infinite Power Solutions THINERGY® microenergy cells (MECs) (Figure 2). The ultra-thin, postage-stamp-sized microenergy cells are flexible and provide unmatched rechargeability, cycle life, and power performance. They have extremely low self-discharge rates and enable decades of shelf life. In fact, these two devices make energy harvesting practical.

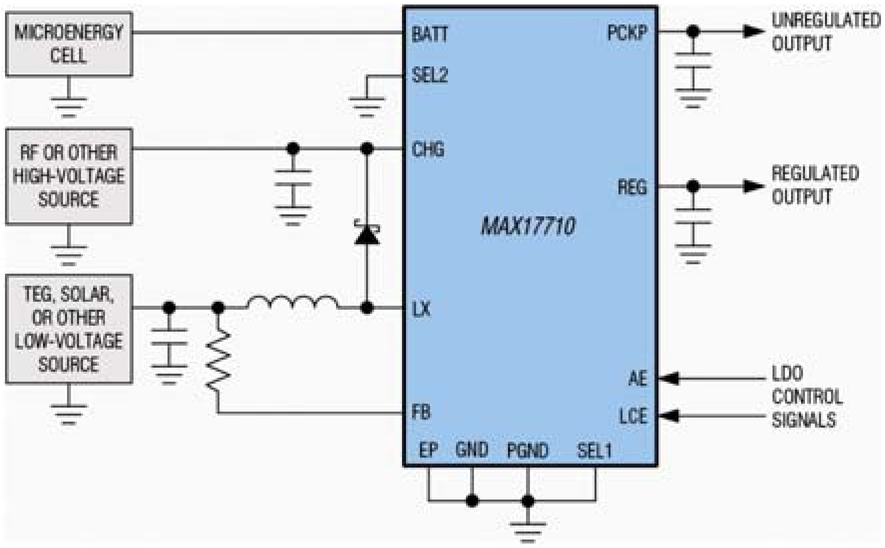

Figure 2: The MAX17710 shown in a typical application circuit harvesting from high-voltage charge sources

The MAX17710 integrates an input boost regulator so it can boost charges from as low as 800mV. It needs no expensive external components to charge an MEC and harvests energy from 1µW to 100mW. To protect the MEC, the MAX17710 handles input source voltages higher than the MEC and regulates or shunts excess power. An ultra-low-quiescent-current, low-dropout linear regulator (LDO) with selectable voltages of 3.3V, 2.3V, or 1.8V prevents potentially damaging overdischarge of the MEC. This also allows the MAX17710 to adapt to a variety of loads, because undervoltage protection recovers only when an external energy source raises the voltage of the MEC back into a safe zone.

Temperature extremes are another concern. At very low temperatures, all batteries exhibit increased characteristic impedance which limits high pulse currents to the application loads. The MAX17710 integrates a unique feature that manages an external storage capacitor in order to provide high pulse currents.

Conclusion

Energy harvesting solutions allow electronics to operate where there is no conventional power source and without the need to run wires or make frequent visits to replace batteries. Using unconventional power sources, the energy-harvesting circuit manages the power generated and protects the energy storage device. Since the energy source is not always present, the energy harvesting system also needs to store the energy.

Energy-harvesting applications are poised to expand rapidly. Some applications are in development that will demonstrate how practical, efficient, cost-efficient, and “clean” energy harvesting is. It is clear that each new implementation with a microenergy cell is going to need some energy-harvesting charger and protection circuit like the MAX17710.

Maxim is a registered trademark and ResourceSmart is a trademark and registered service mark of Maxim Integrated Products, Inc. THINERGY is a registered trademark of Infinite Power Solutions, Inc.

www.maxim-ic.com

High Efficiency Server

Power Solutions for Data Centre and Cloud Computing Applications Move Closer to Production

High efficiency cabinet or rack-level architecture power solutions are necessary to improve the overall power efficiency of systems that perform the increasing number of data centre and cloud computing applications. Power architectures such as IDT's coolRAC include an AC/AC PSU front end, backplane, AC/DC Synchronous Rectifiers, and DC/DC VRM. Such systems demonstrate near 90% overall efficiency.

By Daniel Lenskold, Sr. Manager Strategic Business Development and Marketing; Integrated Device Technology Inc.

Since introducing an initial concept one year ago, IDT has now completed the first system-ready prototypes of its coolRAC components. These include a 480VAC 3-phase input/50VAC output PSU Silverbox, 300W 50VAC input/5VDC output Synchronous Rectifier, and a 5VDC input/1VDC output Voltage Regulator Module (VRM). A 3.6kW Server Power Demonstration System shows the functionality of the power conversion components in a server-like application. This article describes IDT's coolRAC demonstration system and its performance in supporting the global need for higher efficiency in data centre and cloud computing applications.

The coolRAC Demonstration System consists of a 20U 19" standard rack, two PSU Silverboxes, and six power blades (five with 5V loads and one with VRMs and 1V loads). The backplane was designed to show that a low cost two-layer, two ounce copper PCB backplane was sufficient to supply the required power at high efficiency for this demonstration. A LabVIEW interface was used to monitor power at critical points in the system and to control the PSU and blade system configuration and power levels.

VRM

Beginning at the end of the power chain, or the point-of-load conversion, the core voltage conversion is done by a VR12.x Intel standard or equivalent, 6-phase PWM Buck controller. It is widely known that if the input voltage to the controller is reduced from 12V to 5V a significant boost in efficiency can be realised. The efficiency boost achieved versus the typical 12VDC to 1.0VDC conversion is ~3%. The 5VDC to 1VDC VRM was designed using coupled inductor technology. In addition to high efficiency, this approach significantly reduces the need for output bulk capacitors and reduces overall solution size.

Picture 1: coolRAC Demonstration System

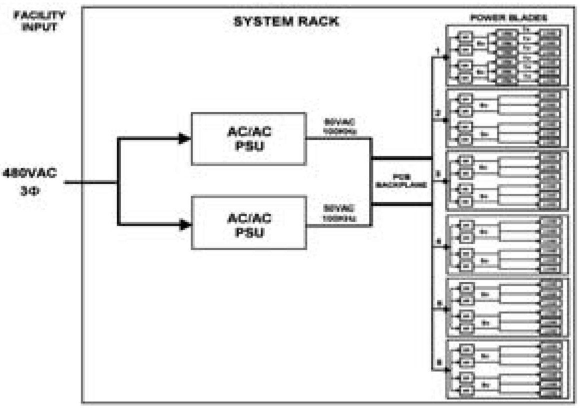

Figure 1: Demonstration System Block Diagram

The point-of-load conversion could also be achieved using a Voltage Regulator Down (VRD) implementation if the board area and the design expertise are available. The coolRAC demonstration system utilises six VRMs on one of the power blades in order to show the overall system efficiency, to the 1VDC output of the VRM. The efficiency of all six VRMs running in parallel on this blade is over 95%

Synchronous Rectifier

The 300W Synchronous Rectifiers (SR) should reside as close to the load (i.e. processor, memory, ASIC, etc) as possible. This is recommended in order to minimize the I2R losses, and to achieve the highest efficiency possible, on the 5VDC (SR output) bus. The SR converts the 50VAC 100KHz backplane voltage to 5VDC at 98% efficiency. The SR configuration is centre tap with secondary side control using a 10:1:1 transformer ratio.

Backplane

Backplane losses are very low using a 50VAC 100kHz AC distribution voltage - typically less than 1%. Also, 50VAC is overall much safer than technologies such as 400VDC or 48VDC distribution. 50VAC was chosen as a safe operating level that also provided very low losses on the backplane. For higher power solutions, additional layers of copper can be added, the backplane voltage can be increased, or a combination of the two can be implemented.

Power Supply Unit/Silver box

The Front-end PSU Silver box was designed for 3.6kW maximum output power. This power level provides a building block for sat-

Power Your Recognition Instantly

Based in Munich, Germany, ITPR Information-Travels Public Relations is a full-service consultancy with over a decade of experience in the electronics sector.
As a small exclusive agency, we offer extremely high ROI, no-nonsense flexibility and highest priority to only a handful of companies.

Strategical Support

Corporate/Product Positioning, Market/Competitive Analysis, PR Programs, Roadmaps, Media Training, Business Development, Partnerships, Channel Marketing, Online Marketing

Tactical PR

Writing: Press Releases, Feature Articles, Commentaries, Case Studies, White Papers
Organizing: Media Briefings, Road Shows, Product Placements in Reviews and Market Overviews, Exhibitions, Press Conferences
Monitoring and Research: Speaking Opportunities, Editorial Calendars, Feature Placement, Media Coverage, Competitive Analysis
Translations: Releases, By-Lined Articles, Websites, etc.

Call or contact us today for a free consultation on how PR can dramatically affect your company's bottom line.

ITPR Information-Travels Public Relations
Stefanusstrasse 6a, 82166 Gräfelfing-Munich, Germany
Tel ++49 (89) 898687-20, Fax ++49 (89) 898687-21,
electronics@information-travels.com

www.information-travels.com

itpr.

APEC® 2012

February 5–9, 2012

Disney's Coronado Springs Resort
Orlando, FL

THE PREMIER GLOBAL EVENT IN POWER ELECTRONICS™

Visit the Apec 2012 web site for the latest information!

www.apec-conf.org

SPONSORED BY

pels

psma power sources manufacturers association

IAS IEEE INDUSTRY APPLICATIONS SOCIETY

isfying the power requirements of much larger systems and is similar to the power level of PSUs for 12VDC and 48VDC architectures. The Vienna 3-phase rectifier PFC front-end, using power MOSFETs provides a .99 power factor at full power. IDT's coolRAC technology allows for current sharing between multiple PSUs and provides power supply redundancy. Both the PSUs and the power blades are Hot-Swappable – a 'must have' for this type of application. The input voltage to the PSU is 480VAC 3-phase, which is readily available in data centre and cloud computing environments. The output is 50VAC 100KHz and the form factor will be somewhat smaller than standard 12V or 48V silver boxes. The 50VAC 100KHz output current waveform is sinusoidal and therefore unlikely to cause problematic system EMI issues. Voltage ripple is a very low 260mVpp. Crucially, the implementation of high efficiency server power solutions in data centres should not require a modification to the existing building infrastructure, as is the case for High Voltage DC distribution.

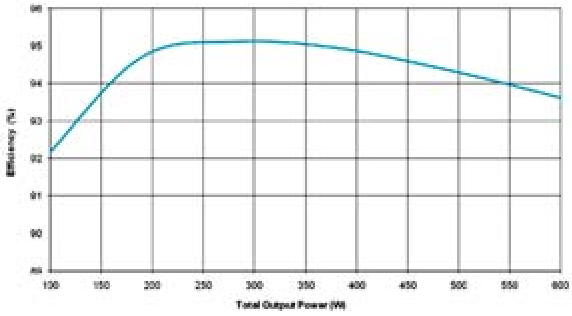

Figure 2: VRM Blade Efficiency (All six VRMs on Blade 1)

Depending on the region of the world 480VAC, 380VAC, 220VAC, 208VAC are already available in data centres.

The closest comparison to the legacy 12VDC and 48VDC PSUs and the coolRAC PSU is to look at the efficiency from 480VAC to the 5VDC output of the SR. One should then factor in the distribution losses of the legacy architectures. The coolRAC efficiency from 480VAC to 5VDC (includes silverbox, backplane losses, and SR) is over 94%. When typical backplane losses in legacy systems are taken into account this is equivalent to 80Plus Titanium level efficiency.

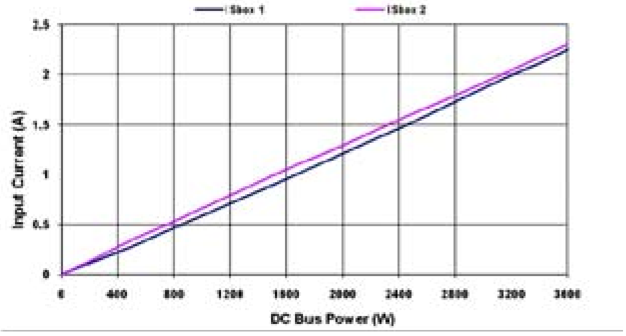

Figure 3: Current sharing <4% across the load range

Overall System

The net effect of having a high efficiency VRM, SR, backplane, and front-end is overall efficiency from 480VAC to 1VDC of almost 90%.

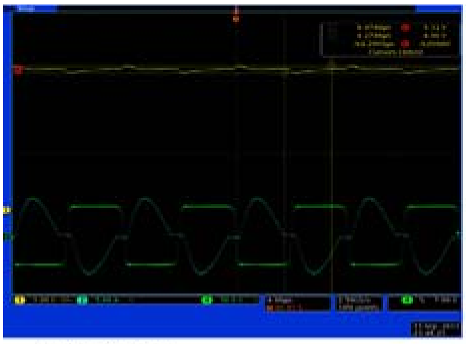

- Loaded Condition
- CH1 = 5VDC Ripple - 260mVpp (measured on blade motherboard test pins)
- CH2 = HFAC Current (measured on SR primary)
- CH4 = HFAC Voltage (measured on backplane)

Figure 4: CH2 (Blue) is 50VAC Generator Output Waveform

Typical server systems today have an overall efficiency that ranges from around 70% to 85%. Most use 220VAC and a 12VDC or 48VDC backplane distribution voltage. The replacement of all existing servers with higher efficiency architectures could save a 12MW data centre approximately $1M per year in electricity costs for power and cooling. The worldwide power consumption for data centres is equivalent to seventeen 1GW power plants (Koomey, Lawrence Berkeley National Laboratory-2007). Assuming a 10% average system power saving implemented worldwide, this would be equivalent to a savings of 141 12MW data centres or in monetary terms, $141M per year.

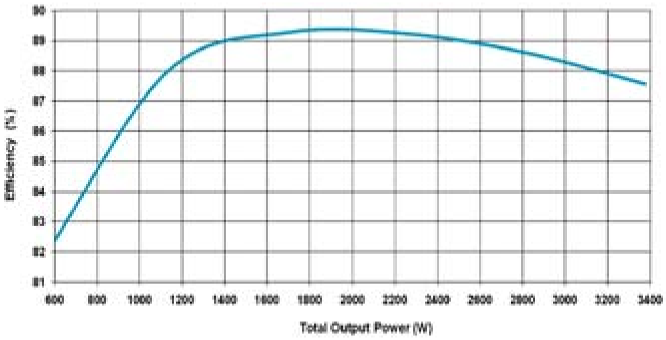

Figure 5: Total System Efficiency from 480VAC to 1VDC

Conclusion

Barring a significant downturn in the world economy, data centre power consumption is expected to increase by 19% over the next 12 months and will continue to increase in the foreseeable future. Market drivers include cloud computing, video and music file sharing, mobile data, and social networking applications.

The potential costs savings that can be achieved with the use of high efficiency server power solutions is extremely high. The higher efficiency also results in the ability to add additional computing resources for the same amount of overall power and cooling. It is common that utilities will charge a significant kilowatt-hour price premium if the allotted power usage for the data centre is exceeded. High efficiency server power solutions allow data centre managers the ability to meet both their power budgets and computing resource requirements.

Architectures such as IDT's coolRAC provide a very attractive option for lowering the cost of operating a data centre and provide improvement to key performance metrics, including gigaflops/watt, that show the effectiveness of power delivery. Such architectures provide a straightforward and cost effective approach to improving power efficiency, meeting today's challenges and positioning for further enhancements.

www.idt.com

10
years
2003–2012
we are the future

Safety Testing Includes 60601-1 Edition 3 Medical Standard

TDK-Lambda UK, a group company of the TDK Corporation, announces that its scope for safety testing has recently been updated to include the Third Edition of 60601-1, the new safety standard for Medical Devices.

The power supply manufacturer has actively participated in the Underwriters Laboratories® Inc. (UL) ‘Clients Test Data Program’ (CTDP) and the IECEE CB Scheme SMT (Supervised Manufacturer’s Test) Program, which is now also under the supervision of UL, for over 16 years. Being on these programs allows TDK-Lambda to use its own testing facilities to generate UL and CB safety reports and test data, this capability helps to reduce time and the accompanying costs for the safety approvals of its own AC-DC power supplies and DC-DC converters.

“As a leading, global power supply manufacturer, it is imperative for us to be at the forefront of safety standards testing,” says Bob Taylor, Safety Engineering Manager at TDK-Lambda UK. “Being approved to the Third Edition of 60601-1 for Medical Devices helps ensure that our latest medical power supplies are tested and approved to the highest safety standards.”

To get onto these programs, Taylor explains: “UL engineers assess all elements pertaining to safety testing from our laboratory quality program to physical resources, as well as test and measurement equipment. Our testing personnel and procedures to conduct specified tests must also be qualified by UL, who reassess our test lab and personnel on an annual basis.”

www.uk.tdk-lambda.com

70W Buck-Driver Powers Long LED-Strings and Multi-Chip Arrays

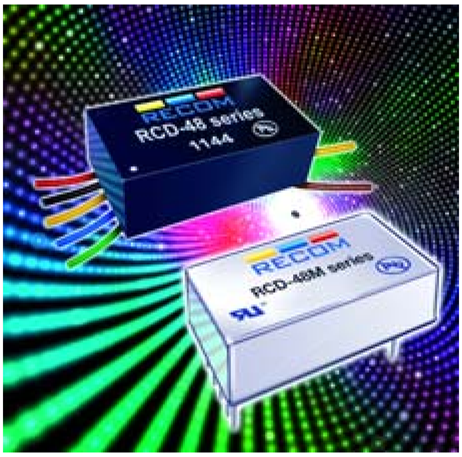

LED lighting is booming! Especially for LED strings and multi-chip arrays, the advance is enormous. The required input voltage for buck-drivers increases with the number of LEDs which have to be supplied with constant current. Currently available models had a limit of approximately 40V. Not so with RECOM’s new RCD-48-family. With input voltage up to 60VDC and constant current outputs of 350, 500, 700 and 1200mA offering device power rating up to 70W. This corresponds to 350W of conventional lighting power! The new buck-driver is ideal for operation with long LED-chains and multi-chip arrays – a real technical achievement!

The RCD-48-drivers are dimmable down to zero with external digital (PWM) or analogue control. The PWM control input can be directly connected to a microcontroller. Efficiency is rated at 96%, with an operating temperature range -40°C and +85°C. The modules are available with pins for PCB mounting or with flying leads for non pcb applications. Whilst the powerful 1200mA version features a metal case, the smaller models are designed in plastic cases. All types are certified to EN/UL-60950-1. The MTBF is specified at MIL-HDBK217F with 1.7 million hours. The warranty is 5 years.

www.recom-electronic.com

Silicon Temperature Sensor Guarantees High Accuracy and Resolution

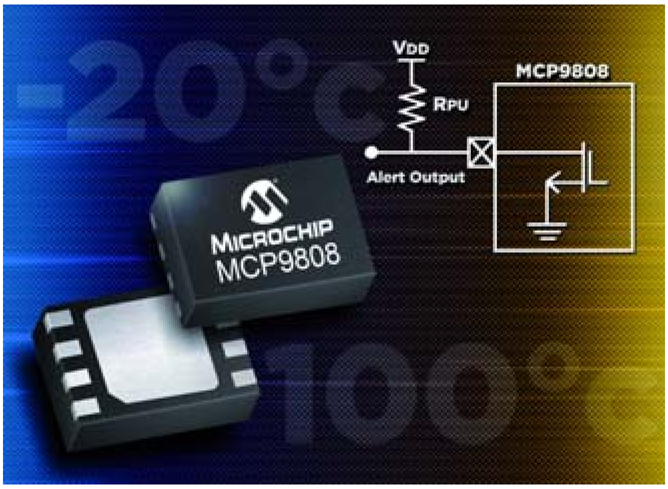

Microchip announces the MCP9808 silicon temperature sensor, which serves a broad range of applications by guaranteeing high accuracy of 0.5 degrees from -20 to +100 degrees Celsius, combined with high temperature resolution of 12 bits (0.0625 degrees Celsius/LSB). The MCP9808 comes in small MSOP and 2x3 mm DFN 8-pin packages, for space-constrained applications, and additional features include shutdown, an under/over-temperature monitor and a critical-temperature alert.

The combination of one of the industry’s highest accuracy silicon temperature sensors with the MCP9808’s wide range of features provides the flexibility for designers to optimise systems for high accuracy over a wide range of temperatures. These applications include thermostats operating at -20 to +45°C; personal computers operating at +85°C and industrial or automotive applications which have an operating temperature of up to +125°C.

www.microchip.com/get/DPHN

Color TFT-LCD Modules with Industry-Leading High Brightness

Mitsubishi Electric is introducing its 7.0” WVGA and 10.6” WXGA color TFT-LCD modules for industrial use. The products are equipped with a built-in LED driver featuring an industry-leading super high brightness of 1000cd/m2 and a super wide viewing angle of 170 degrees both vertically and horizontally making them suitable for use in digital signage or marine applications.

The AA070MC01 and AA106TA01 feature a super wide viewing angle of 170 degrees (horizontal/vertical) which is among the widest in the industry and a clear display enabled by a 1000:1 high contrast ratio with very good visibility. With a super high brightness of 1000cd/m2 they offer excellent performance even in bright illuminated outdoor environments.

The TFT-LCD modules with market leading long-life LED backlight performance can be operated without an inverter achieving a more compact system design and a better cost effectiveness in customer’s applications. At 25 degrees Celsius, LED backlights have an operating life time of at least 100,000 hours.

The TFT-LCD modules achieve a top level wide operating temperature range from -30 degrees to 80 degrees Celsius. Therefore, the models can be implemented in applications in rugged outdoor environments.

With the new TFT-LCD modules Mitsubishi Electric is responding to the increased demand for super high brightness and long operational lifetime color TFT-LCD modules. These characteristics are especially required for applications like digital signage and marine equipment which are exposed to severe temperature environments and strong ambient light.

http://global.mitsubishielectric.com

www.MitsubishiElectric.de

Control IC Reduces Noise Sensitivity for Electronic Ballast and SMPS Applications

International Rectifier has introduced the IRS2500S µPFC™ power factor correction (PFC) control IC for switch mode power supply (SMPS), LED drivers, fluorescent and HID electronic ballast applications.

The IRS2500S µPFC controller can be configured to operate in critical conduction boost PFC or flyback configuration. The new device also features a total harmonic distortion (THD) optimization circuit to reduce line current harmonics. The controller has high noise immunity, simplifying design and reducing system cost.

The IRS2500S PFC control IC expands IR’s existing SMPS and general lighting device portfolios. The new device reduces noise sensitivity, eases PCB layout and provides a cost- effective alternative to existing solutions.

Available in an SO-8 package, the IRS2500S also features micro power start up current of less than 50µA, quiescent current of 2.5mA, drive capability of +800mA/-600mA as well as static and dynamic overvoltage protection and over-current protection. The short minimum on time of the device allows wide input range power factor correction for universal input operation.

Production quantities are available immediately and devices are lead free and RoHS compliant.

www.irf.com

Outstanding High-Linearity Driver Amplifiers

Richardson RFPD, Inc. announces immediate availability of four new high-linearity driver amplifiers from TriQuint Semiconductor. These InGaP / GaAs HBT semiconductor devices deliver high performance across a broad range of frequencies. The TQP7M9101, TQP7M9102, TQP7M9103 and TQP7M9104 are targeted for use in 3G / 4G wireless infrastructure, general purpose wireless, and aerospace & defense systems where high linearity, medium power, and high efficiency are required. This rare combination of high performance makes these devices excellent driver amplifier candidates for both current and next-generation RF transceiver applications.

These innovative RF solutions incorporate on-chip features that differentiate them from other similar products in the market. Each of these amplifiers integrates on-chip DC overvoltage and RF overdrive protection. This feature protects the amplifiers from electrical DC voltage surges and high RF input power levels that may occur in a system. In addition, specially designed on-chip ESD protection allows the amplifiers to have very robust Class 2 (TQP7M9103, TQP7M9102 and TQP7M9103) and Class 1C (TQP7M9104) HBM ESD ratings.

The TQP7M9101, TQP7M9102, TQP7M9103 and TQP7M9104 are available now. To find more information, obtain datasheets, or purchase these products today on the Richardson RFPD website, please visit the TriQuint Semiconductor High Linearity Amplifiers page at

www.rell.com/newdrivers

wwww.richardsonrfpd.com

20~60 W High Efficiency Medical Power Supplies

CUI Inc announced an addition to its high density, high efficiency VMS medical power supply portfolio with the release of three new series ranging from 20 W to 60 W. The units are compact, with footprints measuring 2.38 x 1.60”, 3.00 x 2.00”, and 4.00 x 2.00” for the 20 W, 40 W, and 60 W models respectively.

The VMS series is designed to be used in a wide variety of medical and dental applications, carrying UL/cUL and TUV 60601-1 safety certifications and EN55011 class B EMI compliance. Featuring no-load power draw of less than 0.5 W and efficiency up to 90%, the series is also designed for applications seeking to reduce stand-by and overall power consumption.

The VMS series offers universal input (90-264 Vac) and is available in 7 output voltage models ranging from 3.3 to 48 Vdc. The series can operate from 0° to 50° C at full load, derating linearly to 50% load at 70°C.

Features of the VMS series include overvoltage and short circuit protections.

“The VMS-20, 40 and 60 series are the latest release in what will be a quickly expanding medical power portfolio for CUI,” stated Kraig Kawada, CUI’s Director of Product Management. “We intend to merge the latest in green power technology with the exacting design requirements of our medical customers to develop a range of cutting-edge products specifically for this rapidly growing field,” concluded Kawada.

www.cui.com

Bright LED Technology Thanks to Correct Resistors

LED technology is becoming an increasingly popular choice for lighting up the headlights of modern cars as well as their displays and cockpits. Special resistors are necessary to make the diodes work properly.

LED (light emitting diode) technology provides automotive suppliers with a challenge: The rear part of the light unit leaves only little space for installation and the law requires a minimum brightness level. On top of that, LED chains must not emit different brightness levels and the technology has to withstand high temperatures up to 125 °C. Consequently, resistors used in LED technology have to be very small, perform extremely well, be extraordinarily robust, highly stable and have a small tolerance. Isabellenhütte’s VMK resistors have the required specifications:

- 1 Watt permanent power up to 110 °C terminal temperatureConstant current up to 10 A (10 mOhm)
- Small size (1206; 3.2 x 1.6 mm)
- High pulse loadability (1 W)
- High long-term stability (0.1 % drift in 2,000 h)
- Component assembly: reflow and IR soldering
- TC < 20 ppm/K (temperature coefficient)
- AEC-Q200 certified

Long side termination alternative

Isabellenhütte’s VLK resistors with long side termination are also used in LED technology. At a size of 0612 (3.25 mm length, 1.52 mm width), they also provide particularly high performance and use little space. The contacts on the long side make the component less susceptible to temperature and load cycles.

Specifications at a glance:

- Low resistance starting from 1 mOhm
- 1 Watt permanent power up to 140 °C terminal temperature
- Constant current up to 30 A (1 mOhm)
- Small size (0612)
- High pulse loadability (1 W)
- High long-term stability (0.1 % drift in 2,000 h)
- Component assembly: reflow and IR soldering
- AEC-Q200 certified

www.isabellenhuette.de

Encapsulated ac-dc Power Supplies

CUI Inc announced the release of five new series of encapsulated ac-dc power supplies ranging from 5 W to 25 W. The board mount VSK series is compact, measuring 2.0” x 1.0” x 0.6” in the 5 W package. With efficiency reaching 87% and an operating temperature range of -25 to 70 °C, these isolated ac-dc modules are ideally suited for use in low power ITE, industrial, and consumer electronics applications where board space is a concern.

The VSK series provides continuous output power, universal input (85-264 Vac), and are offered in fully regulated dc outputs of 3.3, 5, 9, 12, 15, 24, and 48 Vdc. The class II ac-dc modules carry UL/cUL 60950-1 certifications as well as the CE mark. Protections for over voltage, over temperature, and short circuit conditions are included. Additionally, the modules offer 4K Vac isolation in the 5 and 10 W versions and 3 K Vac isolation in the 15, 20, and 25 W versions. The VSK series is available immediately through Digi-Key with prices starting at $13.56 for 100 pcs. Please contact CUI for OEM pricing.

www.cui.com

Ultrafast Charging in Smartphones and Tablets with Programmable Flexibilty

Summit Microelectronics has expanded its fourth-generation family of programmable Li-Ion battery charger integrated circuits (ICs) with the introduction of two new products. The SMB346 and SMB347 deliver up to 2.5A charge/system current with dual input/dual output CurrentPath™ technology for operation with a dead or missing battery. Dual inputs accept both USB and AC/DC with automatic selection and support for all battery charging standards: USB 2.0 specification, USB on-the-go supplement, USB battery charging specification 1.2, IEEE1725 standard, Chinese USB charging specification, and others. Furthermore, the SMB346 and SMB347 are the only battery charger ICs with CurrentPath™ to detect the input source type (USB host/hub/charger, AC/DC, etc.) and automatically optimize operation for the fastest and safest battery charging.

The SMB346 and SMB347 are based on a 3MHz, switch-mode DC-DC architecture, with minimal external components, which allows for over 90 % efficient conversion and extremely compact solution size.

The devices enable fast charging due to higher charge currents, while reduced thermal dissipation improves user comfort, system reliability and Green operation (www.summitmicro.com/MobileGreen).

Furthermore, Summit’s proprietary TurboCharge™ patent-pending technology enables high charge current, even from relatively low-power sources (example: up to 750mA output from 500mA USB source). As consumer devices continue to employ larger batteries, the SMB346 and SMB347 reduce charge time for consumer convenience.

The SMB346 and SMB347 are ideal for a wide range of portable devices such as smartphones, tablets, digital still cameras, digital camcorders, wireless routers, portable media/MP3 players (PMP), portable GPS navigation equipment, and portable game consoles/controllers.

www.summitmicro.com

High Capacitance, Low profile, Panel Mount Capacitors for EMI Filtering

Syfer, has announced the availability of a number of important extensions to its already wide range of solder-in panel mount EMI filters. Advanced in-house research and development has resulted in the introduction of a series of discoidal capacitor versions, which offer the advantage of high capacitance values, up to several microfarads, in a compact and robust package.

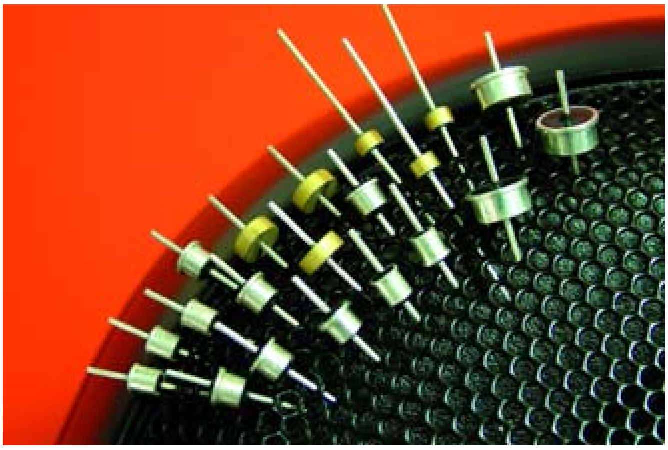

Ideal as low-profile, panel mount filters, the SFSS devices are constructed with a discoidal capacitor soldered to a feedthrough pin. They are offered with a choice of C0G/NP0 or X7R ceramic dielectrics. Available in 5 different diameters (2.3mm, 2.8mm, 3mm, 5mm and 8.75mm), capacitance values range from 10pF to an impressive 2.2µF. Working voltages range from 50V to 3kV and operating temperature range is -55 to 125oC. These devices are able to withstand a solder-in temperature of 250oC.

Syfer maintains its global reputation for performance, offering the highest voltage and capacitance for any given size. For designers looking for space saving solutions, Syfer’s solder-in EMI filter ranges allow the specification of smaller parts when compared to competitive offerings. Custom devices can also be produced on request.

Aimed primarily at manufacturers of EMI filters, these low cost, yet robust and reliable devices will also meet the demands of equipment manufacturers in the communications, industrial, military/aerospace and sensors markets.

The SFSS discoidal series joins the existing SFSR, SFST and SFSU ranges of feedthrough EMI filters for soldering direct to a chassis or panel, suitable for hole diameters of 2.9mm, 3.5mm and 5.8mm respectively. Featuring a metal body and epoxy encapsulation, they offer superior filtering performance in a robust package. Working voltages are from 50Vdc to 500Vdc.

Manufactured in the UK at Syfer’s Norwich facility, these fully RoHS compliant capacitors are available immediately on an 8 to 14 week lead time, depending on the quantity and specification ordered.

www.syfer.com

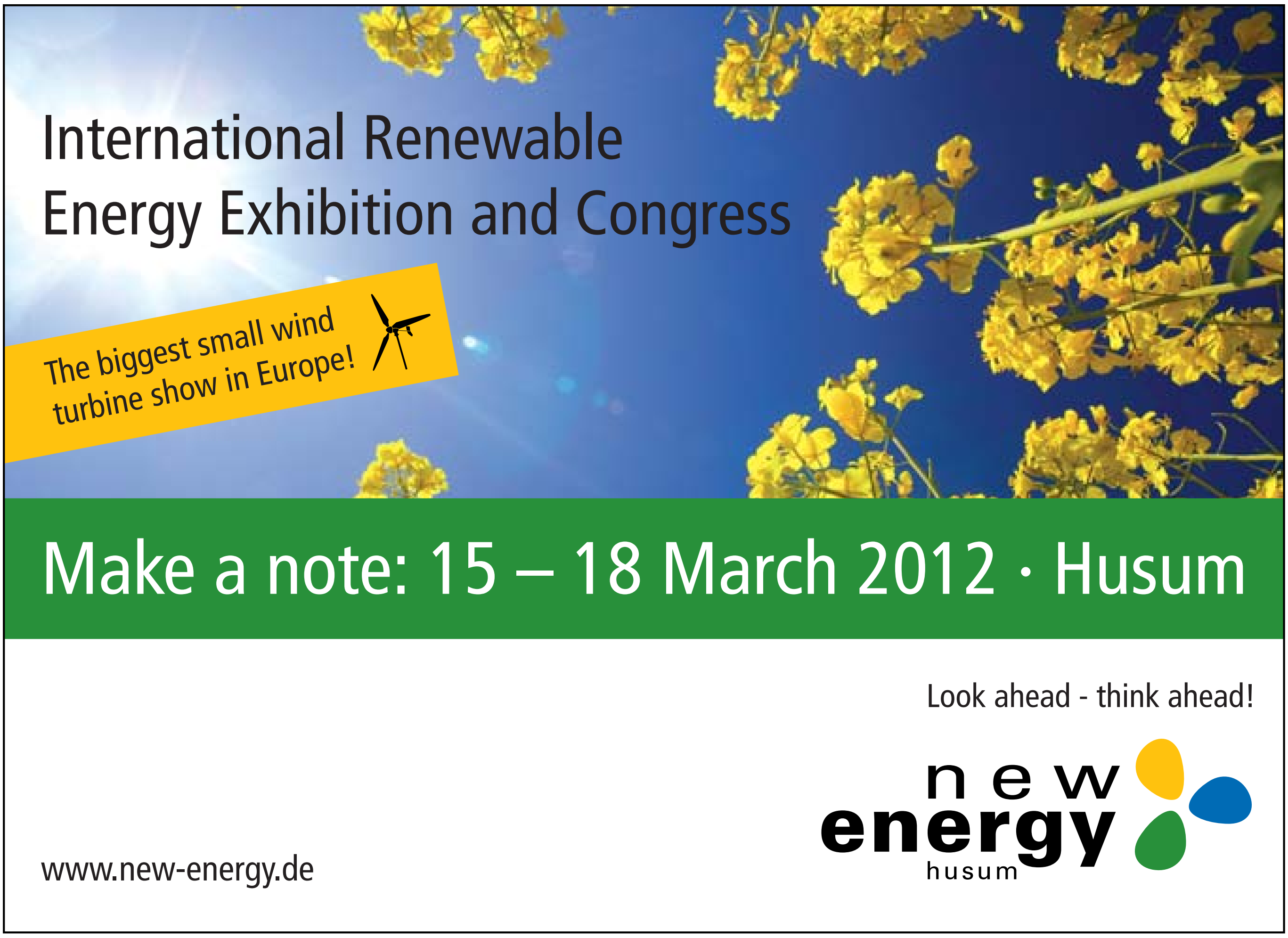

Silicon Carbide Power Devices In Chip Form

Cree continues to advance the revolution in high-efficiency power electronics with the release of the industry’s first fully qualified SiC MOSFET power devices in “bare die” or chip form for use in power electronics modules. Cree’s SiC Z-FET™ MOSFETs and diodes are used in advanced power electronics circuits to achieve significantly higher levels of energy efficiency than is possible with conventional silicon devices.

Power modules typically combine a number of discrete power switching devices – MOSFETs and diodes – in a single integrated package for high-voltage power electronics applications such as three-phase industrial power supplies, telecom power systems and power inverters for solar and wind energy systems. In traditional MOSFET packaging technologies, the parasitic inductance of the long leads can limit the switching capability of SiC MOSFETs. By offering Cree customers bare die alternatives, circuit designers can now take full advantage of the switching performance of SiC technology by reducing the effects of the package-parasitic inductance.

“With the availability of fully qualified SiC MOSFETs as unpackaged chips, manufacturers of power modules can realize the performance advantages of SiC devices—better high temperature operation, higher switching frequencies and lower switching losses – without the limitations imposed by conventional plastic packaging of discrete devices,” explained Cengiz Balkas, Cree vice president and general manager, power and RF. “The design advantages of implementing SiC power devices in power electronic modules include the ability to achieve higher current and voltage ratings with fewer components, which in turn can enable maximum power density and increased reliability.”

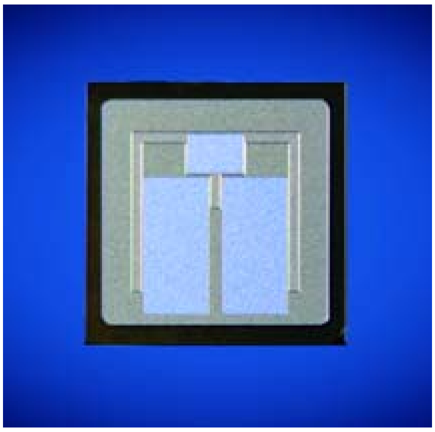

www.cree.com/power

Web-Based Software Package to Select the Optimum Multilayer Capacitor

Just announced by Europe's leading MLCC manufacturer, Syfer Technology, is a web-based software package called CapCad™, the software tool is easy and fast to use, and provides circuit designers with a readily accessible capacitor comparison facility. CapCad™ includes SPICE models with various parameter values that reflect typical performance at the chosen frequencies. Importantly, engineers can select the temperature range relevant to the application, and adjust it as necessary, to note how it may affect the expected performance of the design.

In operation, the user has the ability to plot 2-port Scattering Parameters, Impedance, Q Factor or Equivalent Capacitance over any frequency span from 1MHz to 40GHz. CapCad™ also includes a Smith Chart utility, plus the S-Parameter data can be copied and converted in Touchstone format (s2p). The modelling software supports Syfer's High Q range of multilayer capacitor devices. It can be used to compare several devices at one time, and allows designers to model the cumulative effect of multiple devices in one design.

Although the data presented by CapCad™ cannot be construed as a specification or guarantee of actual performance, it is based on calculated models to represent typical performance. Device modelling is regarded by engineers as a useful application development tool, particularly for high frequency products being designed into complex applications. CapCad™ is an important element in Syfer's customer design and development support programme.

The software tool is available free of charge, downloadable from the company website at

www.syfer.com

Common Mode Power Line Choke for Ultra-Slim Products

With the WE-CMBH series Würth Elektronik now also offers a common mode power line choke in a horizontal version. With a profile height of only 22 mm the power line choke is ideal for slim housings.

Due to low-capacitance winding technology, suppression over a wide band is now possible. This makes the WE-CMBH an excellent choice for interference suppression in the frequency range from 150 kHz to 30 MHz. The product is available with inductance values from 1 mH up to 7 mH with a nominal current of up to 10 A.

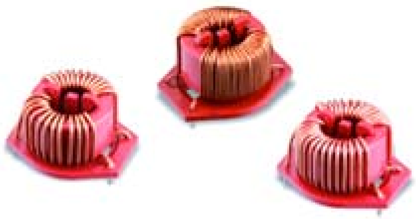

In power electronics the WE-CMBH is used as power filter and output filter as well as in motor interference suppression.

Würth Elektronik specifies the operating temperature range as –40 to +125 °C.

The components are available ex stock. Samples are provided free of charge.

www.we-online.com

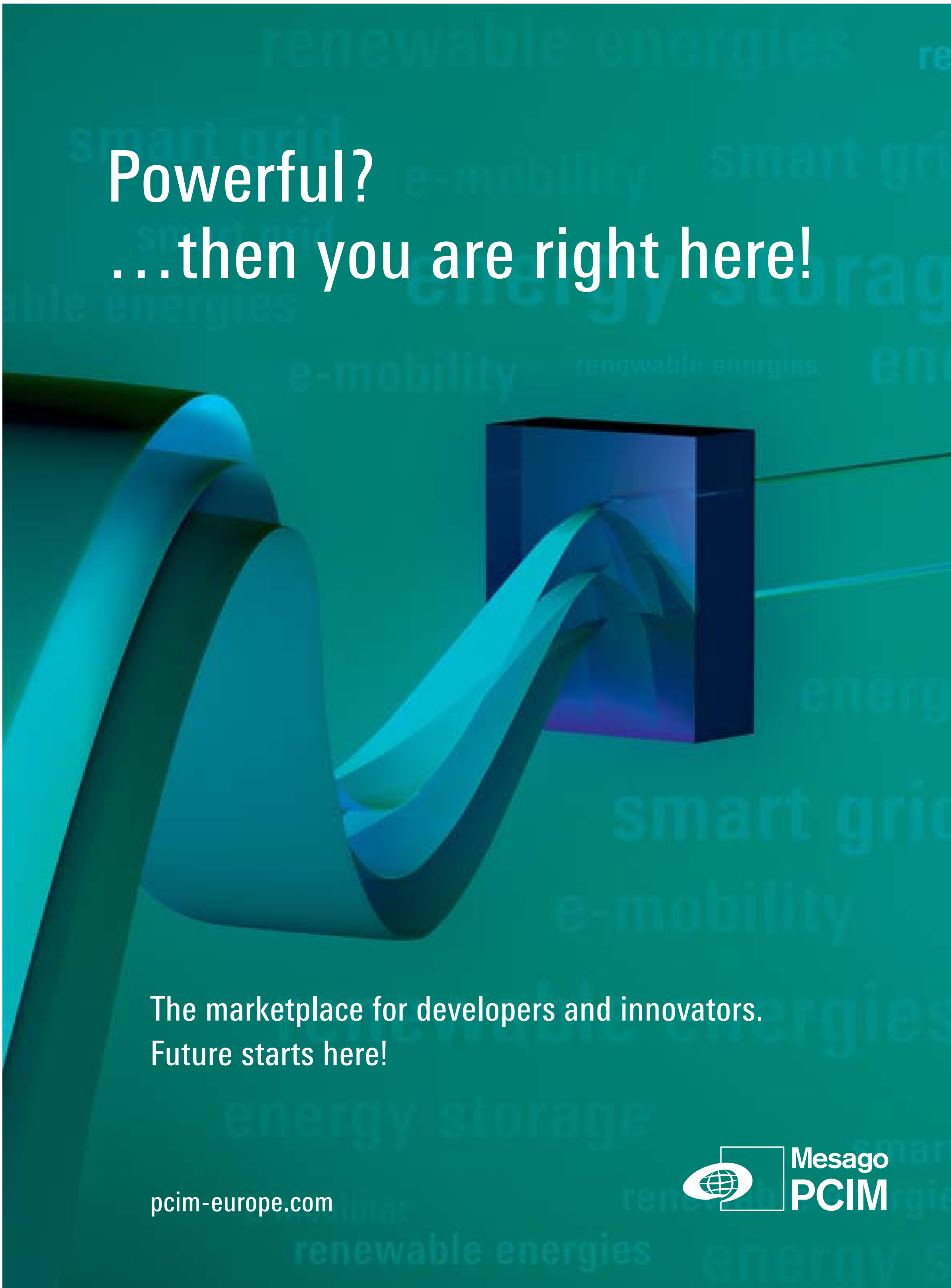
renewable energies
smart grid
e-mobility
energy storage
renewable energies
smart grid
e-mobility
renewable energies
energy storage

Industry’s Lowest Supply Voltages and Power Consumption

Intersil Corporation has developed a series of single, dual and quad digitally controlled potentiometers (DCPs) featuring the industry’s lowest supply voltages, power consumption and noise.

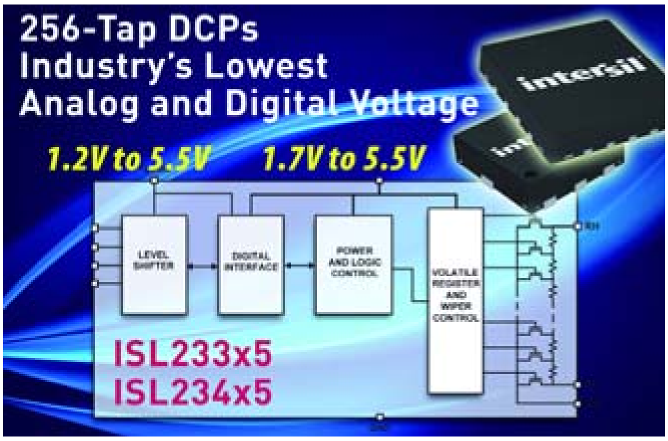

The ISL233x5 and ISL234x5 provide the most flexible and reliable solution wherever a voltage or resistor setting is needed. Supply current is as low as 2.8uA at 5V, which is 40% to 50% lower than most competitive devices. Analog supply voltage can range from 1.7V to 5.5V. The digital supply voltage may be even lower at 1.2V to 5.5V, eliminating the need for a level shifter if the MCU has low voltage digital interface outputs. Users can control the wiper position through either the I2C or SPI interface.

The ESD tolerance is a robust 6.5kV HBM, and the DCPs are offered in leaded packages for easy debugging as well as tiny microTQFN packages for space-constrained applications. Devices may be ordered with 10kOhm, 50kOhm or 100kOhm total resistances. They are designed for use as three-terminal potentiometers or as two-terminal variable resistors in portable medical instrumentation, network cards, smartphones, regulator margining and other applications requiring calibration or digital control.

www.intersil.com

Highest-Density 6-A Power Module With Integrated Inductor

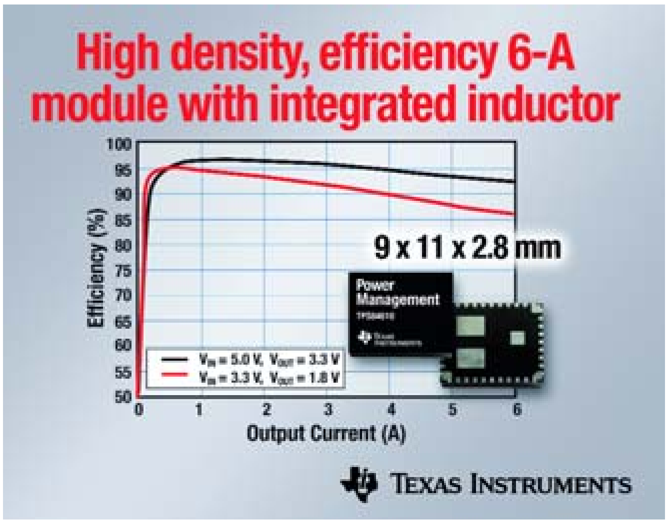

Texas Instruments introduced a 6-V, 6-A synchronous integrated power module with integrated inductor, which achieves an industry-best 750 watts per cubic inch and peak power efficiency up to 97 percent. The TPS84610 provides excellent thermal performance of 12°C/W, which is 40-percent better than competing modules. The device simplifies telecom power designs for DSPs and FPGAs by combining the inductor and passives onto one lead frame, requiring only three external components for a complete, easy-to-design 150-mm2 solution. For samples and evaluation module visit: www.ti.com/tps84k-preu.

The TPS84610 supports input voltages from 2.95 V to 6 V, generates a low 0.8-V output and has an adjustable switching frequency from 500 kHz to 2 MHz. The 9-mm x 11-mm x 2.8-mm low-noise module meets EN55022 Class B electromagnetic emissions, allowing it to support noise-sensitive applications, such as broadband communications equipment.

www.ti.com

ADVERTISING INDEX

Standard
Technology
SKiN
Technology

Extend Battery Life With IR's Benchmark MOSFETs

Small Power MOSFETs Designed for Handheld Devices

Gate Drive - 4.5V Optimized, 2.5V Capable, 12V Maximum

BV_{DSS}	Package	Max. $R_{DS(on)}$ @ 4.5V (mΩ)	Max. $R_{DS(on)}$ @ 2.5V (mΩ)	Part Numbers
-20V	PQFN 2x2	31	53	IRLHS2242
	SOT-23	54	95	IRLML2244
20V	PQFN 2x2	11.7	15.5	IRLHS6242
	SOT-23	21	27	IRLML6244
	Dual PQFN 2x2	45	62	IRLHS6276
30V	PQFN 2x2	16	20	IRLHS6342
	TSOP-6	17.5	22	IRLTS6342
	SOT-23	29	37	IRLML6344
	Dual PQFN 2x2	63	82	IRLHS6376

Gate Drive - 10V Optimized, 4.5V Capable, 20V maximum

BV_{DSS}	Package	Max. $R_{DS(on)}$ @ 10V (mΩ)	Max. $R_{DS(on)}$ @ 4.5V (mΩ)	Part Numbers
-30V	PQFN 2x2	37	60	IRFHS9301
	SOT-23	64	103	IRLML9301
	Dual PQFN 2x2	170	290	IRFHS9351
25V	PQFN 2x2	13	21	IRFHS8242
	SOT-23	24	41	IRFML8244
30V	PQFN 2x2	16	25	IRFHS8342
	TSOP-6	19	29	IRFTS8342
	SOT-23	27	40	IRLML0030

Features

- Available in both N & P Channel for simple design
- Latest silicon technology offering low $R_{DS(on)}$ for increased battery life
- 2.5V drive capable available for 1-cell Li-Ion Battery Applications
- PQFN package offers high power density reducing system size

Applications

- DC Load Switch
- Battery Protection
- DC-DC Converter
- Screen Backlight Boost Converter

Your FIRST CHOICE for Performance

For more information call +49 (0) 6102 884 311
or visit us at www.irf.com

International
IOR Rectifier
THE POWER MANAGEMENT LEADER